ADVANCED MATERIALS
www.advmat.de

Bacteria-Responsive Nanostructured Drug Delivery Systems for Targeted Antimicrobial Therapy

Guillermo Landa, Gracia Mendoza, Silvia Irusta, and Manuel Arruebo**

Bacteria exhibit adaptive phenotypic traits that confer resistance to host defenses and antimicrobial therapies. In response to the global threat of antimicrobial resistance, bacteria-responsive nanostructured drug delivery systems have emerged as a promising alternative to conventional broad-spectrum antimicrobials. These systems release therapeutics selectively in response to bacterial presence or to their secreted enzymes, toxins, antigens, or extracellular biomarkers, enabling precise activation at infection sites while minimizing off-target effects. Bacterial components such as membrane proteins, signaling molecules, biofilm-associated glycolipids, and enzymes (e.g., lipase, hyaluronidase) serve as triggers for these smart carriers. Exopolysaccharides are also commonly targeted using nanocarriers with complementary recognition elements. Such systems are often surface-modified or loaded with antimicrobials for on-demand release. Benefits include enhanced selectivity, reduced side effects, improved biofilm penetration, higher intracellular accumulation, and potential for personalized therapy. A variety of materials—including lipid-based carriers, metal nanoparticles, polymer nanoparticles, and inorganic nanomaterials—have been engineered to release antimicrobials only in the presence of pathogenic bacteria, often offering dual therapeutic effects (e.g., anti-inflammatory). Furthermore, many platforms integrate multiple antimicrobial mechanisms, reducing the likelihood of resistance development. This review highlights recent preclinical studies validating bacteria-responsive nanosystems and underscores their advantages over passive drug delivery and conventional free antimicrobials.

1. Introduction

Antibiotics represent one of the most significant medical breakthroughs of the last century. They have reduced the mortality in communicable diseases (e.g., tuberculosis, respiratory and healthcare-associated bacterial infections, etc.), in endogenous diseases (e.g., sepsis, urinary tract infections, skin and soft tissue infections, etc.), and thanks to their prophylactic use, in many standard procedures (e.g., wound management, burns, joint replacements, C-sections, surgeries, etc.).[1] However, antimicrobial resistance (AMR) represents one of the main threats to human health, food security, and development. It is estimated that by 2050 antimicrobial resistance will cause up to 1.91 million deaths attributable to AMR and 8.22 million deaths associated with AMR.[2] The Centers for Disease Control and Prevention's 2019 Antibiotics Resistant Threats Report showed that in the US at least one infection was accounted for every 11 seconds and one death every 15 min from antibiotic-resistant bacteria and fungi.[3] Despite all the preventive campaigns to reduce the use and misuse of antibiotics, AMR still represents a tremendous burden for healthcare systems. It has been reported that the use of antibiotics in 76 low, medium, and high-income countries studied over 16 years (2000-2015) increased 65% (expressed as prescribed daily doses), and the antibiotic consumption rate increased 39%.[4] However, several recent promising reports have demonstrated inspiring strategies to reverse antibiotic resistance. For instance, inhibitors of the expression of genes associated with AMR have demonstrated encouraging results in vivo in preclinical models.[5] In

G. Landa, S. Irusta, M. Arruebo
Instituto de Nanociencia y Materiales de Aragón (INMA)
CSIC-Universidad de Zaragoza
Zaragoza 50009, Spain
E-mail: arruebom@unizar.es

The ORCID identification number(s) for the author(s) of this article can be found under https://doi.org/10.1002/adma.202510355

DOI: 10.1002/adma.202510355

G. Landa, S. Irusta, M. Arruebo
Department of Chemical and Environmental Engineering
University of Zaragoza
Campus Río Ebro-Edificio I+D, C/ Poeta Mariano Esquillor S/N,
Zaragoza 50018, Spain

G. Landa, G. Mendoza, S. Irusta, M. Arruebo
Health Research Institute Aragon (IIS Aragon)
Zaragoza 50009, Spain
E-mail: gmendoza@iisaragon.es

G. Mendoza
Department of Pharmacology
Physiology
and Legal and Forensic Medicine, Facultad de Medicina-Edificio A
University of Zaragoza
C/Domingo Miral, S/N, Zaragoza 50009, Spain

addition, colistin-resistant and multidrug-resistant *Acinetobacter baumannii* infections in vivo have been eradicated using synthetic antimicrobial polypeptide-based polymers, opening new avenues in this field.[6]

Biofilm formation represents another hurdle to the host immune response and to pharmacological antimicrobial treatments, including antibiotics and antiseptics. Planktonic bacteria rearrange in a complex symbiotic medium mainly composed of extracellular polysaccharides, proteins, lipids, and DNA, which attaches to both biotic and abiotic surfaces, forming a dynamic, coordinated functional multicellular community named biofilm. The information about the surface to which bacteria are attached is also genetically transmitted to their descendants to be evolutionarily more efficient in colonizing that same surface.[7] Biofilm formation responds to an adaptive developmental response to environmental stress (temperature, pH, antibiotic treatment, etc.) changing their phenotypic growth rate and genetic transcription. For instance, bacterial biofilms are from 10 to 1000 times more resistant to conventional antibiotics than their planktonic counterparts.[8] In addition, many pathogenic biofilms are polymicrobial in nature increasing their tolerance to antibiotic regimes.[9] Tissue debridement, antibiotic combination therapies, quorum sensing (QS) inhibitors, biofilm dispersant agents are therefore recommended when treating bacterial biofilms. Biological therapies represent another alternative in their treatment including the use of phages and their released enzymes,[10] antimicrobial peptides secreted by eukaryotic cells,[11] human monoclonal antibodies,[12] cationic antimicrobial peptides,[13] and so on, reverting in some cases the bacterial sessile phenotype to an antibiotic-sensitive planktonic state.

AMR bacterial strains are microbiologically detected using culture-based techniques (e.g., disk diffusion method, agar dilution testing, broth microdilution, Gram-staining, chromogenic screening plates, etc.), and also different automated systems are accessible in many clinical settings, including Matrix-Assisted Laser Desorption Ionization-Time of Flight Mass Spectrometry (MALDI-TOF MS), polymerase chain reaction (PCR), enzyme-linked immunosorbent assay (ELISA), DNA microarrays, DNA chips, loop-mediated isothermal amplification (LAMP), next-generation sequencing, etc.[14,15] The presence of bacterial biofilms is diagnosed using clinical guidelines. In its guideline, the European Society of Clinical Microbiology and Infectious Diseases highlights different clinical and microbiological laboratory-derived indicators to aid in the diagnosis of biofilm-forming bacteria. These indicators include common signs of infection, medical records of biofilm-predisposing conditions, long-lasting infections (>7 days), antibiotic-treatment failure, and recurrence, etc. Biofilms are routinely identified microscopically, using culture and non-culture-based techniques (PCR) and using specific immune responses to already identified bacteria.[16]

Considering the challenges posed by AMR and biofilm formation, innovative solutions are essential for the development of advanced treatment strategies. The application of materials with at least one dimension below 100 nm in the biomedical field constitutes the field of Nanomedicine. Scientific and clinical research in this area is principally directed toward cancer management and antimicrobial therapies. Various nanotechnological approaches have been developed not only to monitor the presence or absence of bacterial pathogens in both sessile and planktonic states, but also to abrogate AMR bacteria, to prevent biofilm formation, and to treat already formed mature biofilms. In this regard, several metallic nanomaterials (e.g., silver, copper, zinc, gold nanoparticles, etc.) show multiple mechanisms of action against prokaryotic cells, and consequently, with their use, the chances of developing antimicrobial resistance decrease.[17] Metal nanoparticles (NPs) have also shown inhibitory biofilm-forming ability against different Gram-positive and Gram-negative bacteria.[18] Nanocarriers of different nature (i.e., polymers, liposomes, solid lipid nanoparticles, micelles, polymersomes, etc.) are also commonly used in antimicrobial therapies to protect the antimicrobial cargo from degradation and act as reservoirs to provide a sustained release of drug, preventing suboptimal antibiotic doses and the consequent AMR appearance. Therefore, the nanoparticulate encapsulating material is used to control the release kinetics of the antibiotic or antiseptic loaded in their interior, and thanks to their large surface area per volume ratio, their bioavailability and activity are increased compared to their micro- and macroscopic counterparts. In addition, combination therapies (e.g., antibiotics/metal NPs,[19] antimicrobial peptides/metal NPs) have demonstrated synergetic effects when tackling AMR.[20] Metallic nanomaterials are also used in different antimicrobial treatments based on photodynamic therapy, generating locally reactive oxygen species from tissue oxygen after light irradiation, eliminating pathogenic bacteria and preventing biofouling in what is called antimicrobial photodynamic therapy (aPDT). NPs have also been commonly used to protect organic photosensitizers from photobleaching to facilitate aPDT. Photothermal ablation of antibiotic-resistant strains and biofilm eradication have been reported as other examples of the benefits of using different nanomaterials in the antimicrobial field.[21,22] Again, combination therapies based on different approaches have recently been used to combat infection and avoid drug resistance. For instance, NPs acting as photosensitizers in aPDT have been combined with QS inhibitors in vivo using multimodal nanoparticulated platforms.[23] Multiple pathologies can also be treated using multifunctional nano-based platforms. For instance, anti-inflammatory, antitumoral, antibacterial, and regenerative properties have been reported for silicon-based hybrid nanofibrous scaffolds containing curcumin and polydopamine in murine models of *Staphylococcus aureus*-infected wounds.[24]

The use of nanomaterials in biosensing to detect the presence or absence of sessile or planktonic bacteria and to outperform current antibiotic susceptibility tests is out of the scope of this review. However, it is worth mentioning those nano-based approaches allow monitoring of real-time infection and treatment progression. In this regard, fluorescent imaging of infected wounds in response to the presence of specific bacteria has been reported using toxins and enzymes secreted by bacteria that trigger the lysis of NPs containing fluorescent dyes.[25] Reporter wound dressings composed of lipidic nanovesicles that switch on a fluorescent color when in contact with pathogenic wound biofilms have been reported using an *ex vivo* porcine skin model of burn-associated wound infection.[26]

In this review, we are interested in compiling the most recent and significant work describing the use of nanostructured materials to treat and detect pathogenic bacterial infection, but focusing exclusively on those systems having responsive ability under the presence of bacteria. Hence, on-demand nanostructured

systems that detect and eradicate AMR and biofilm forming bacteria will be reviewed selecting those systems that respond solely when bacteria are present thanks to the use of specific triggers such as surface antigens or receptors or specific enzymes, toxins, extracellular biomarkers, acidic cues, signaling molecules, adhesins, antimicrobial peptides, proteases, DNAses, glycoside hydrolases, glycolipids, and so on. Compared to passive or continuous drug delivery methods, the main advantages derived from the use of bacteria-responsive nanoparticulated drug-containing carriers include enhanced selectivity, reduced side effects, improved biofilm penetration, superior antimicrobial intracellular accumulation, and potential for personalized therapy tailored to individual patient needs. The release of the antimicrobial drug only when pathogenic bacteria is present favors a rationale usage of antimicrobials, prevents under- or overdosing, and aligns with the dynamics of the infection, enhancing the therapeutic outcome.

2. Targeted and Triggered Strategies

Targeted and stimuli-responsive nanocarriers enable precise drug release at infection sites, reducing off-target effects and enhancing therapeutic efficacy. This section summarizes commonly employed strategies for both targeting and triggering, focusing on how nanomaterials exploit infection-associated cues—such as acidic pH, bacterial enzymes, metabolites, and redox imbalances—to achieve selective delivery and a controlled release of antimicrobial agents. These approaches offer promising solutions to address antibiotic resistance and biofilm-associated infections.

2.1. Bacterial Targets to Boost Triggered Release of Bactericidal Compounds

Prior to the development of novel bactericidal strategies, the selection of the target must fulfil certain requirements. First, the target—both physiological and pathological—should be common, conserved, and key in bacteria, while at the same time being different and not essential in animals and/or humans. Moreover, the characteristics, function, and location of the target should be well-known and distinct from other targets to facilitate the accessibility and identification of its corresponding targeting moiety, as well as to prevent cross-resistance.[27]

For example, the secretory (Sec) pathway meets these requirements being highly conserved in bacteria and controlling its essential functions such as nutrient and drug uptake, metabolism, and cell defense. Among the wide variety of membrane proteins that involve the Sec pathway, SecA and the type I signal peptidase (SPase I) have been widely explored as a potential target for antimicrobials, as they are essential for bacterial survival. SecA is ubiquitous and capable of interacting with different ligands (e.g., nucleotides, signal peptides), promoting ATPase activity and, thus, protein translocation and conformational changes that result in its de-insertion from the membrane.[27] Its potential as an efficient target resides mainly in its location, as it can be found as both cytoplasmic and peripheral membrane proteins, depending on its catalytic cycle. Moreover, it has been recently reported its function as an ion and protein-conducting channel, making it more accessible for targeting. In fact, some studies have shown its versatility due to its multiple interactions and enzymatic actions, along with the reduction in bacterial virulence after targeting SecA, which confines defective virulence proteins that would otherwise be refluxed by SecA.[27,28] The most important strategies to effectively target SecA are the inhibition of its ATPase activity and its translocation. In this regard, some authors have developed in vitro assays with moderate results, though some of them have shown the potential of different inhibitors.[29,30] On the other hand, SPase I promotes the release of mature proteins from the cell membrane to achieve their final destination, whether cellular or extracellular. Its function is essential for the release of precursors and controls different secretion processes.[31] SPase I expression shows differences between Gram-negative and Gram-positive bacteria, being critical for bacterial viability only in the former. Moreover, its conformation also differs, presenting one amino-terminal transmembrane segment in Gram-positive bacteria, whereas Gram-negative bacteria exhibit more than one. SPase I is ubiquitous and accessible to inhibitors due to its location in the outer layers of the membrane. Its inhibition results in bacterial death owing to the accumulation of preproteins in the membrane. SPase I exhibits different key actions depending on the bacterial strains, though the most widespread role is its involvement in pathogenesis.[27] **Figure 1** shows a schematic representation of the targets that advanced nanotherapies can be directed to. A summary of several other bacterial targets is included in **Table 1**.

2.2. Key Targets in Bacteria Populations: Biofilm and Quorum Sensing

Biofilms, or sessile bacterial populations, are the most widespread in vivo living forms in which bacteria attach to a surface—whether biotic or abiotic—and secrete extracellular polymeric substances (EPS). Bacteria become confined within this polymeric matrix and are organized into populations with functional heterogeneity, exhibiting social behavior and cell communication to phenotypically adapt to their environment and associated potential stressors.[43] The EPS not only protects cells from these external threats, including antibiotic penetration, but also creates a microenvironment in which the development of AMR can increase considerably.[44] Biofilms also serve as reservoirs for planktonic bacteria that may be released and colonize and infect other surfaces. Owing to these characteristics, these sessile bacterial populations are the source of several chronic infections. EPS is essential for the different stages of biofilm formation: adhesion, early formation, maturation, and dispersal. The differential targeting of any of these stages would be a successful strategy to prevent biofilm formation or to eradicate mature biofilms. Targeting EPS synthesis and/or secretion, as well as the adhesins that facilitate the interaction between the host surface and bacteria, are key strategies for eliminating biofilms.[45] The widespread conservation of the second messenger cyclic di-GMP (c-di-GMP), along with its critical role in biofilm synthesis, makes its inhibition an attractive approach to hamper biofilm formation and QS. In fact, seven inhibitors of c-di-GMP synthesis have been shown to be effective in impeding biofilm formation in *Vibrio cholerae* ΔVC1086, and one of them

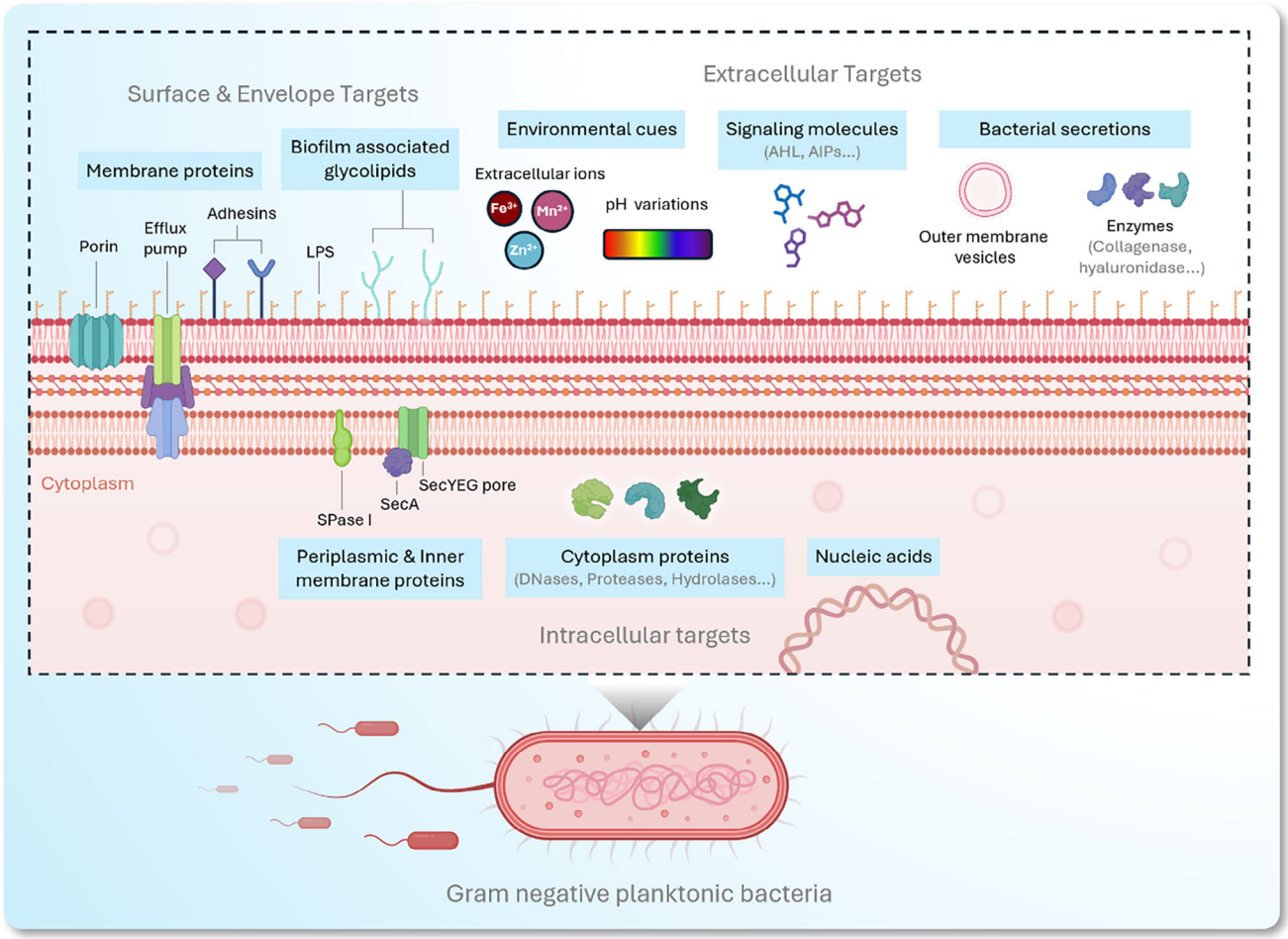

Figure 1. Classification of bacterial targets that can be addressed by advanced nanotherapeutic strategies, grouped into surface and envelope targets, extracellular and intracellular targets.

Table 1. Summary of different targets reported for planktonic and sessile bacteria.

Target	Location	Effects	Refs.
SecA	Cytoplasmic and peripheral membrane	Inhibition of ATPase activity or translocation	[27–29]
SPase I	Anchored to the membrane by one (Gram-positive bacteria) or more amino-terminal transmembrane segments (Gram-negative bacteria)	Inhibition of precursors release and secretion processes	[27]
Bacterial physiology	Whole cell and environment	Metabolism disruption and/or inhibition of pathogenic action	[32]
AHL	Whole cell and environment	Disruption of bacteria signaling and biofilm structure	[33–35]
AIP	Environment	Disruption of QS in *S. aureus* through the formation of the complex AgrC-AgrA and inhibition of biofilm dispersal	[36,37]
c-di-GMP	Whole cell and environment	Inhibition of biofilm formation and QS	[38,39]
Adhesin secretion	Whole cell	Inhibition of host surface-bacteria interaction	[40,41]
AMPs	Whole cell and environment	Inhibition of persisters	[39]
Iron chemical structural analogues	Whole cell and environment	Inhibition of iron-mediated mechanisms in bacteria surveillance and biofilm formation (i.e., siderophore action)	[39,42]
Proteases, DNases and glycoside hydrolases	Environment	Degradation of Extracellular polymeric substances (EPS) making biofilms more susceptible to antimicrobials	[39]

has also been effective in inhibiting biofilm formation in *Pseudomonas aeruginosa* (*P. aeruginosa*) PAO1.[38] Mannosides have also been identified as effective inhibitors of adhesin secretion in catheter-associated urinary tract infections (UTIs) caused by *Escherichia coli* (*E. coli*) UTI89.[40,41,46]

Proteases, DNases, and glycoside hydrolases that mediate EPS degradation are also relevant targets to facilitate biofilm dispersion and revert bacteria to their susceptible planktonic state. A wide variety of proteases have been described that inhibit biofilm generation, degrade preformed biofilms, and make biofilms more susceptible to antimicrobial effects.[39] Moreover, DNases can act on extracellular DNA, which has been defined as a scaffold for biofilm formation. Several DNases have been shown to be active in deconstructing biofilms, especially in the early stages of biofilm formation. However, the emergence of resistance to DNases highlights the need to combine this approach with other EPS degradation strategies.[39,47,48] Finally, endolysins and other families of hydrolases have been demonstrated to efficiently remove biofilms, even against polymicrobial biofilms in murine models of chronically infected wounds.[39,49,50]

Interference with iron metabolism is by far the key approach to disrupting the metabolic state of bacteria. Bacterial survival, as well as biofilm formation and dispersion, are highly influenced by iron-mediated pathways. Therefore, chemical structural non-canonical iron analogues can be assimilated by bacteria, even if they do not fulfil iron functions, thus hampering iron-mediated pathways. In this context, gallium has been the most widely used analogue to inhibit the bacterial mechanisms that depend on iron.[39,42] Gallium, specifically Ga^{3+}, as a similar ionic radius and chemical properties of iron has, can be recognized by bacterial iron transport systems and incorporated into iron-dependent pathways. However, unlike iron, gallium is unable to undergo redox cycling between Ga^{2+} and Ga^{3+}, a crucial process for many bacterial enzymatic reactions. This results in the disruption of iron-dependent metabolic functions, leading to oxidative stress, impaired respiration, and ultimately bacterial cell death. Due to its multi-target antimicrobial activity, including effectiveness against drug-resistant bacterial strains, Ga^{3+} has attracted considerable interest as a promising antibacterial strategy. To enhance its therapeutic efficacy and overcome its low bioavailability, various Ga^{3+}-based compounds and combination therapies utilizing different forms of Ga^{3+} have been developed.[51] Notably, Ga^{3+} has also been incorporated into nanostructured platforms, such as metallic nanoparticles, to further improve its stability, targeted delivery, and antimicrobial potency.

Targeting dormant cells or persisters may also be a promising approach to inhibit biofilm dispersal, as they can act not only as bacterial reservoirs but also play an active role in drug tolerance. In this regard, antimicrobial peptides (AMPs) are promising agents as broad-spectrum antimicrobials, owing to their high efficacy even at antimicrobial concentrations in some cases lower than those required for antibiotics.[39]

On the other hand, QS plays an important role in regulating biofilm pathogenesis, as it supports cell communication mediated by the generation and detection of signal mediators,[52] which in turn involves the synchronization of gene expression and the acquisition of competitive characteristics to adapt to changes in the microenvironment or to develop resistance. Therefore, targeting QS is also an interesting strategy in the treatment of infections.[17] In this context, acyl-homoserine lactones (AHL) are among the main mediators in Gram-negative bacterial QS. The length and functionalization of the acyl side chain determines the QS activity of AHL; for example, small peptides can control QS-related gene expression in Gram-positive bacteria, while other autoinducers (AI-2) are active in both Gram-positive and Gram-negative bacteria.[35] Furthermore, AHL can alter *P. aeruginosa* PAO1 and PA14 eDNA release, biofilm structure, and the production of EPS,[33,34] whereas the autoinducing peptide AIP can disrupt QS in multiple *Staphylococcus aureus* strains through the complex AgrC-AgrA, thereby altering biofilm dispersal.[36,37] In **Figure 2**, the phases of biofilm formation are shown, along with the various strategies that can be employed to target them at each stage.

3. Nanostructured Materials for Antimicrobials Delivery

Different nanomaterials, organic and inorganic, have been used as carriers for the targeted and triggered release of antimicrobials such as polymeric NPs, solid lipid NPs, liposomes, lipid polymer hybrid NPs, dendrimers, carbon nanotubes, porous silica particles among others.[53] Some of the systems are composed of a combination of inorganic and organic materials because multifunctional nanocomposites have been shown to have the potential to establish new combinations of therapeutic drugs to be used in targeted drug delivery taking advantage of both organic and inorganic materials. The addition of triggerable ability can greatly improve the efficiency of the treatment and minimizes the damage to non-pathological tissues. In **Figure 3**, a diagram of the nanocarriers described in this review is included. The most relevant examples are described in the sequel.

3.1. Lipid-Based Materials

Lipid-based nanocarriers are versatile drug delivery systems known for their ability to improve drug solubility and bioavailability. These nanocarriers can be broadly categorized into lipid vesicles, such as micelles and liposomes, and lipid nanoparticles. The latter group includes standard lipid nanoparticles, solid lipid nanoparticles, featuring a rigid core made of high-melting-point lipids, and nanostructured lipid carriers that combine solid and liquid lipids.

3.1.1. Lipid Vesicles

Lipid vesicles are spherical structures composed of lipid layers. Within this category, micelles and liposomes are the most notable examples. Micelles are spherical aggregates of surfactant molecules, with a hydrophilic head group and a hydrophobic tail group. In contrast, liposomes are spherical vesicles formed by phospholipids, which make up one or more bilayers that surround an aqueous compartment.[54,55] Just as micelles can only encapsulate hydrophobic drugs in their oil-phase core, liposomes facilitate the encapsulation of drugs of a broad nature:

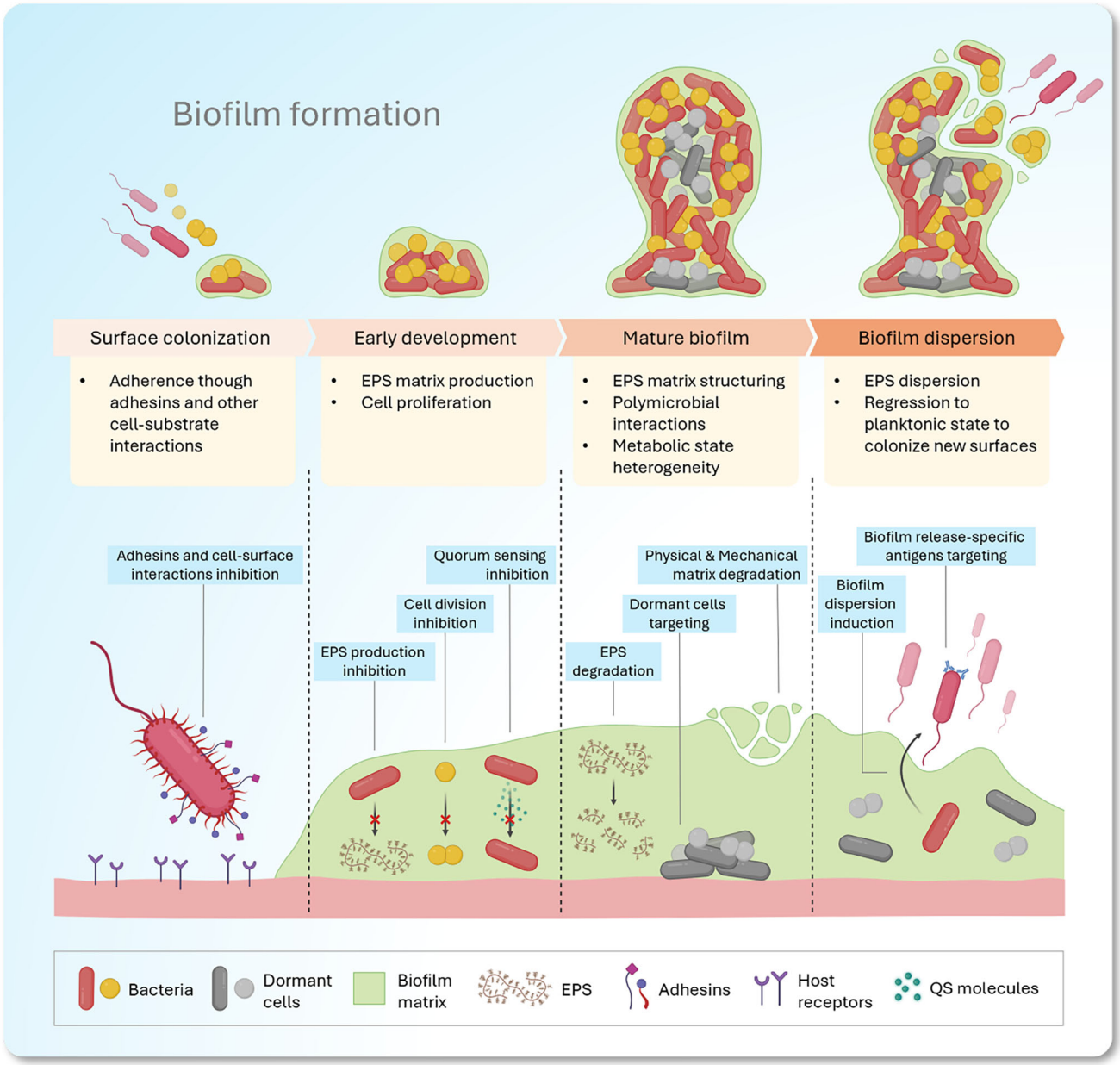

Figure 2. Stages of biofilm formation and targeted therapeutic interventions. The diagram illustrates the stages of biofilm development at the top (*surface colonization, early development, mature biofilm formation, and biofilm dispersion*), each with distinct characteristics of antimicrobial behaviour and structural properties. The bottom section presents therapeutic strategies targeting each stage, including adhesion inhibition, EPS production suppression, QS disruption, biofilm dispersion induction, among others.

hydrophilic compounds in the aqueous interior and hydrophobic or amphiphilic ones in their lipid bilayer. Furthermore, the loading capacity of liposomes tends to be higher than that of micelles.

Lipid vesicles are recognized as the most widely used drug nanocarriers present in clinical practice.[56] As drug delivery systems, they significantly influence the pharmacokinetic/pharmacodynamic (PK/PD) profiles, offering a possibility of gradual and sustained release during the circulation of the drug in the body. Similarly, these formulations protect the drug from degradation and inactivation, expanding its bioavailability, as well as reducing toxic side effects.[57] Lipid vesicles have been intensively studied with a wide spectrum of antimicrobial compounds against chronic bacterial infections. Bacterial strains resistant to a specific antibiotic have increased their susceptibility to the same antibiotic when included in a lipid vesicle formulation, compared to its administration in its free form.[58–61] In addition, liposomes exhibit a bilayer structure like that of cellular membranes, thereby contributing to their fusogenicity.[62] This distinctive ability allows liposomes to fuse with bacterial cell membranes, enabling the direct release of their antimicrobial content

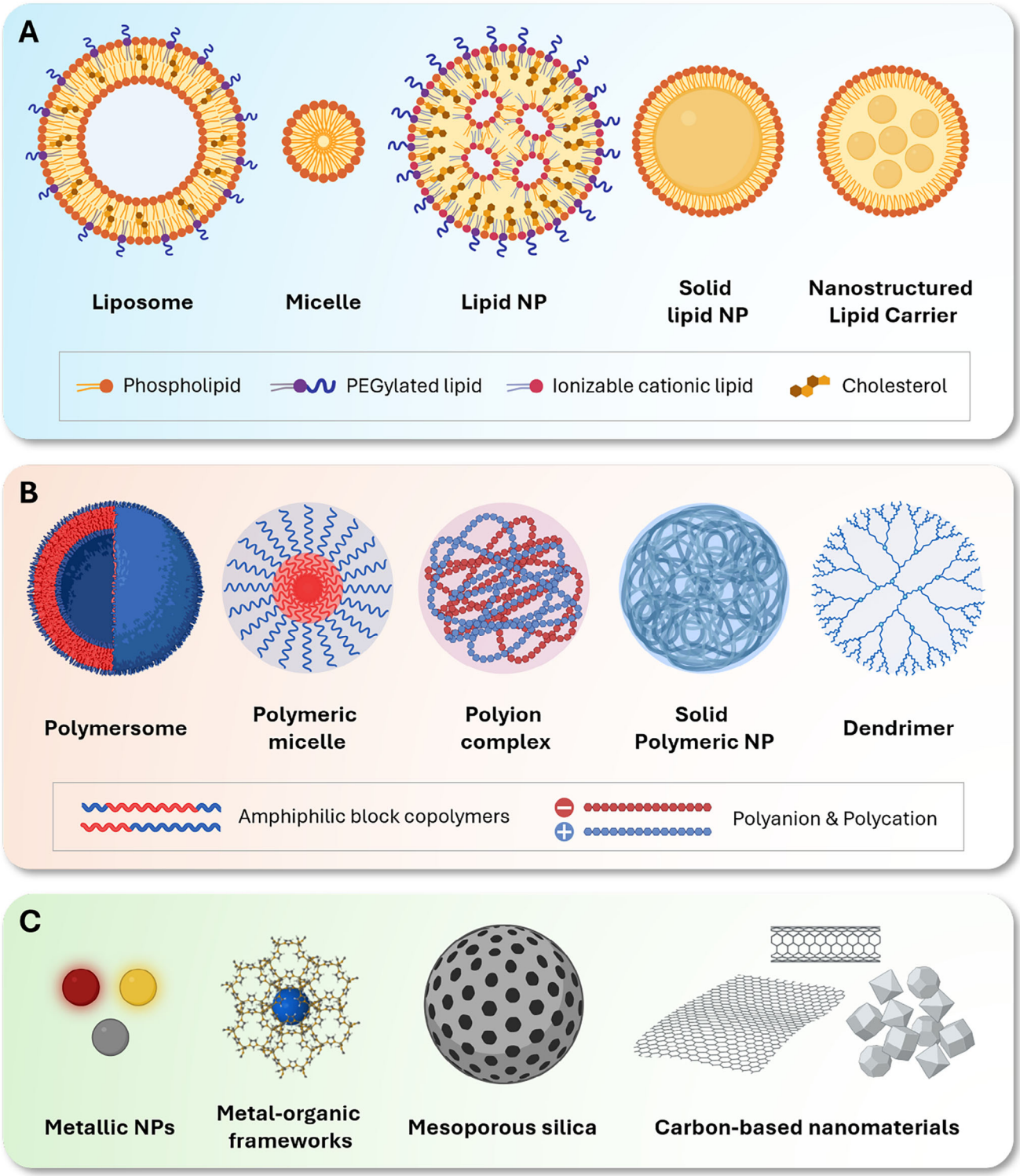

Figure 3. Schematic representations of the main types of nanocarriers used in drug delivery, including lipid-based A), polymeric B), and inorganic C) systems.

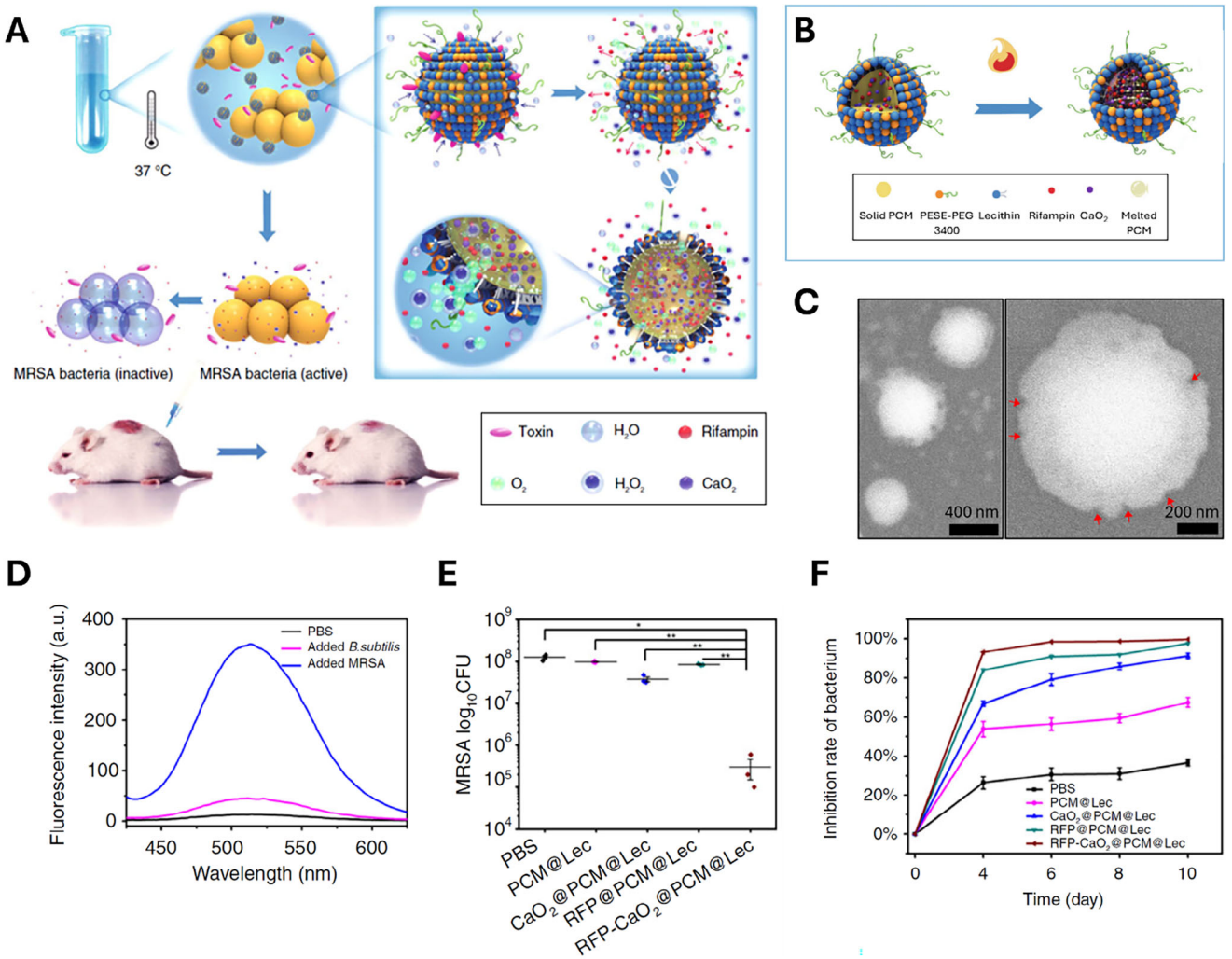

Figure 4. Endogenous stimulus-powered antibiotic release from lipid-based nanoreactors for combination therapy. A) Liposome-based nanoreactors, coated with lecithin, DSPE, and PEG, encapsulate a fatty acid mix containing calcium peroxide and rifampin (RFP-CaO_2@PCM@Lec). Upon contact with bacterial toxins, pores form in the nanoreactor membrane, allowing water to enter. The water reacts with CaO_2 to produce hydrogen peroxide, which partially decomposes into oxygen, triggering rifampin release. B) Composition of the nanoreactors. Internal fatty acids undergo a solid-to-liquid phase transition at 37° C. C) SEM images of toxin forming pores. D) Fluorescence recovery of the encapsulated fluorophore upon its release from liposomes triggered by MRSA (blue), *B. subtilis* (red), and PBS buffer (black). E) Bacterial inhibition rate of MRSA after incubation with 100 μg mL^{-1} of different materials at 37 °C for 2 h. F) In vivo inhibitory efficiency of different treatments, measured as the ratio of bacterial count relative to the initial load in MRSA-infected mouse wounds. $p < 0.05$ (*), $p < 0.01$ (**), $p < 0.001$ (***). Adapted under the terms of the CC-BY 4.0 license.[66] Copyright 2019, Springer Nature.

into the bacterial cells or infected eukaryotic cells.[63,64] Furthermore, liposome-encapsulated antibiotics represent a promising approach for treating biofilm-associated infections. For instance, in the work of Cheow et al., it was shown that liposomes exhibit a strong tendency to adsorb into biofilm surfaces and effectively penetrate the thick mucus layer that surrounds biofilm colonies, making them especially effective for the treatment of chronic lung biofilm-associated infections.[65] The release of antibiotics from those liposomes was triggered by rhamnolipid surfactants, which are glycolipids routinely produced by *P. aeruginosa* to maintain its biofilm architecture.

In the study conducted by Wu et al. an endogenous stimulus-powered targeted delivery system was developed by combining a liposome with phase change materials (PCM) for controllable antibiotic release.[66] Among the virulence factors that pathogenic bacteria possess, bacterial toxins are the ones with the highest selectivity. The α-toxin segregated by *S. aureus* disrupts cells by forming pores in cellular membranes and altering their permeability. The developed reported system took advantage of this toxin to form pores and in situ gas generation that drove the release of antimicrobial agents, as depicted in **Figure 4**. A combination of lauric acid and stearic acid, that melts at human body temperature (melting point at 35.2–38.3 °C), was used to load calcium peroxide and the antibiotic rifampicin. The obtained particles were coated with lecithin and DSPE-PEG3400, forming liposome-based nanoreactors. The bacterial toxins induced pores in the nanoreactors' walls, water molecules entered and reacted with CaO_2 producing hydrogen peroxide that partially

decomposed to oxygen to power the antibiotic release. Meanwhile, the Ca^{2+} increased the concentration of ions inside the liposomes accelerating rifampicin delivery. The bactericidal capacity of those nanoreactors was evaluated in vivo against Methicillin resistant *S. aureus* (MRSA) infection using a murine skin infection model. The wound healing rate in animals treated with the described nanoreactors was significantly higher than that of the control group, showing, in addition, better bacterial inhibition efficiency.

Lastly, leveraging pH changes, the liposome cargo can be released in a controlled manner. In the study by Omolo et al., oleic acid-derived quaternary lipid and parent oleic acid were incorporated into liposomes as pH-responsive components for site-specific antibiotic delivery.[67] The presence of the quaternary lipid and the oleic acid in the lipid bilayer of the liposomes forms an "on and off" switch to release the antibiotic vancomycin from the liposome. Under basic pH, the oleic acid would deprotonate and form a supramolecular complex with the quaternary lipid, and the negative charge would dominate, avoiding antibiotic release. However, in an acidic environment, oleic acid would be protonated, losing its charge, resulting in a slight repulsion between the positively charged quaternary lipid and thus, leading to drug release due to this rearrangement. The pH-responsive liposomes had superior activity in vitro, both at pH 7.4 and pH 6.0, when compared to equivalent doses of vancomycin alone. In vivo studies showed that the amount of methicillin-resistant *Staphylococcus aureus* (MRSA) collected from mice treated with the formulations was ≈190 and 6.33-fold lower than that retrieved from the untreated groups and from free vancomycin-treated mice, respectively.

Despite their numerous advantages, lipid vesicles have drawbacks both during their synthesis and during their in vivo performance. These drawbacks include low encapsulation efficiency, potential loss of encapsulated drug, oxidative degradation, and instability, which can lead to unwanted premature vesicle rupture or aggregation. The stability of lipid carriers is determined by their lipid composition, as well as pH and temperature. Vesicle stability is significantly more compromised under physiological conditions than under storage conditions and in in vitro studies.[68]

3.1.2. Lipid Particles

Lipid nanoparticles are a versatile class of nanocarriers within the lipid-based drug delivery systems, specifically designed to improve the stability, bioavailability, and controlled release of therapeutic agents. This category includes standard lipid nanoparticles (LNPs), solid lipid nanoparticles (SLNPs), and nanostructured lipid carriers (NLCs), each with distinct structural and compositional characteristics that allow custom applications in drug delivery, including antimicrobial applications targeting bacterial infections and biofilm-related diseases.

Standard LNPs are characterized by a core-shell structure with a unique core of reverse micelles that creates aqueous cavities, intended for encapsulating hydrophilic drugs or nucleic acids. These LNPs are particularly effective for genetic therapies, as they are formulated with cationic ionizable lipids, a key component that enhances the complexation and stabilization of negatively charged therapeutic molecules such as mRNA or siRNA. These ionizable lipids undergo protonation in the intracellular acidic environments, promoting endosomal escape and ensuring efficient intracellular delivery. Standard LNPs have gained prominence in the field of vaccine delivery, notably after the development of mRNA vaccines for COVID-19, where they protect the fragile mRNA and deliver it directly into the cytoplasm of target cells. This mRNA transfection technology is also translatable to the treatment of bacterial infections. Hou et al. demonstrated the potential of LNP-mediated mRNA delivery to address multidrug-resistant (MDR) bacterial infections, specifically in immunocompromised hosts susceptible to sepsis.[69] They hypothesized that the adoptive transfer of macrophages engineered to express AMPs linked to cathepsin B (CatB) could enhance innate immunity, prevent bacterial immune evasion, and eliminate MDR bacteria in septic mice. To validate their hypothesis, they designed AMP-CatB mRNA constructs that include a broad-spectrum antimicrobial peptide, IB367 (AMP-IB367), coupled with CatB via a CatB-sensitive linker. AMP-IB367 has demonstrated rapid bactericidal activity in clinical trials, while CatB, an endogenous lysosomal protein, aids in delivering AMP-IB367 into lysosomes. Using vitamin C-derived LNPs, they transfected macrophages with AMP-CatB mRNA. Once inside the macrophage cytoplasm, the mRNA is translated into the AMP-CatB protein complex, which is then translocated to the lysosomes. In this acidic environment, CatB cleaves the linker, releasing AMP-IB367 to act directly on bacteria. This system is designed to overcome bacterial immune evasion mechanisms, which often protect MDR bacteria from typical phagolysosomal killing. The adoptive transfer of these engineered macrophages enabled the recovery of septic, immunosuppressed mice against infections caused by *S. aureus* ATCC BAA-44 and *E. coli* ATCC BAA-2340.

In contrast, SLNPs are composed of lipids with a high melting point that remain solid at room and physiological temperatures, such as fatty acids, triglycerides, steroids, and waxes.[70] This solid lipid matrix provides an optimal environment for the encapsulation of hydrophobic drugs, offering a stable platform that prevents drug degradation and achieves a sustained release profile. SLNPs have demonstrated effectiveness in encapsulating and delivering poorly soluble antimicrobials, including ciprofloxacin, rifampicin, and tobramycin,[71] which are crucial for treating bacterial infections and penetrating biofilms. Their structure allows SLNPs to act as a diffusion barrier against rapid drug release, enhancing bioavailability while reducing retention in the mononuclear phagocytic system, ultimately increasing drug efficacy and stability over time.[72] However, due to the solid nature of the lipid core, SLNPs are less suited for the encapsulation of hydrophilic drugs, as these compounds are embedded within the lipid matrix rather than within an inner aqueous compartment. NLCs expand on the concept of SLNPs, addressing some of the limitations associated with SLNPs by combining solid and liquid lipids. This approach permits the formation of nanoparticles with a partially lamellar or amorphous lipid core, offering extended drug loading capacity and better stability during storage while maintaining similar low toxicity levels. In the context of bacterial infections and biofilm-targeted therapy, NLCs have demonstrated their potential by improving drug penetration into biofilms and allowing for localized, controlled drug release.[73] Together, these three subclasses of lipid particles represent a

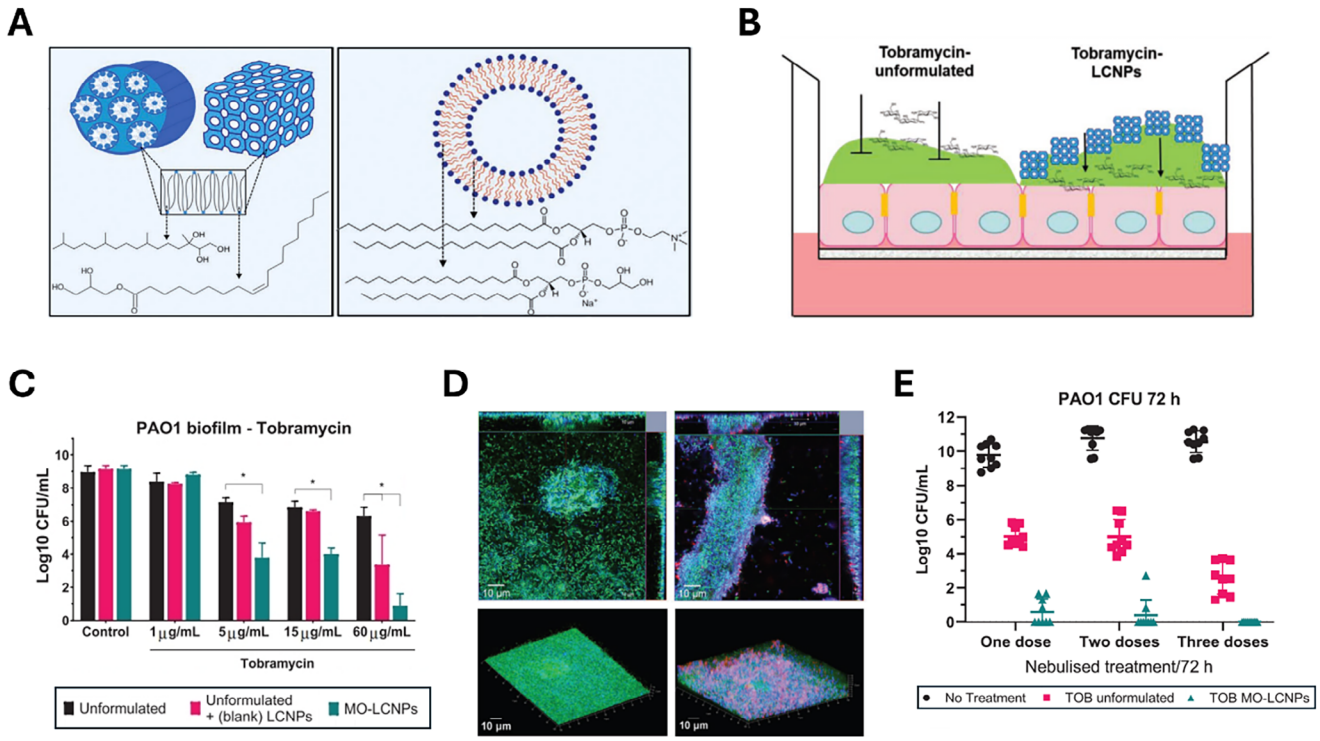

Figure 5. Tobramycin-loaded liquid crystal nanoparticles for eradication of cystic fibrosis-related *P. aeruginosa* biofilms. A) Schematic representation of LCNP internal nanostructures (inverse hexagonal and bicontinuous cubic phases), along with the chemical structures of phytantriol and monoolein (MO). Conventional liposome structures composed of DSPC and DPPG are also illustrated for comparison. B) Scheme depicting the difference in transport efficiency of TOB across biofilm and epithelial barriers when delivered as a free drug versus when encapsulated in LCNPs. C) Antibiofilm activity of TOB delivered as an unformulated solution (black), unformulated TOB combined with drug-free LCNPs (pink), and TOB formulated within MO-LCNPs (teal). Data are shown as mean ± SD ($n = 6$). Statistical analysis by two-way ANOVA ($p < 0.01$). D) Orthogonal and 3D-rendered z-stack confocal microscopy images of *P. aeruginosa* PAO1-GFP biofilms (green) grown in flow cells for 3 days, treated with either unformulated Cy5-labeled TOB (blue) or MO-LCNPs co-loaded with Cy5-TOB (blue) and Rhodamine B (red). E) Therapeutic efficacy of MO-LCNP-encapsulated TOB compared to unformulated TOB in a chronic infection model. Treatments were applied via nebulization using a vibrating mesh nebulizer. Biofilm burden was quantified after one, two, or three treatments over a 72 h period. Reproduced with permission.[75] Copyright 2021, Wiley.

versatile toolkit for addressing challenges in drug delivery. Their varied structures and lipid compositions allow for the encapsulation of a wide range of therapeutic molecules, improve cellular uptake, and offer tunable release profiles, particularly in the treatment of bacterial infections and biofilm-associated diseases. As an example of their efficacy, Kalhapure et al., synthesized SLNPs with a cleavable acetal linkage to deliver vancomycin in the acidic environments of MRSA infection sites.[74] Intradermal injections were used to infect with MRSA Rosenbach (ATCC BAA-1683TM) the space between the epidermal and the subcutaneous layer of mice skin, avoiding the direct entry of the bacteria into systemic circulation. There were significant differences ($p < 0.05$) between the total number of CFU/mL (colony forming units/mL) in MRSA-infected mice treated with vancomycin-loaded particles compared to those treated with unloaded ones. Besides, there was almost a 3-fold reduction in the thickness of the skin treated with loaded particles compared to that treated with unloaded ones due to a greater reduction in the number of bacteria.

In the work of Thorn et al., the efficacy of Tobramycin Liquid Crystal NPs (TOB-LCNPs) in eradicating biofilms formed by *P. aeruginosa* PAO1 was investigated.[75] This research highlights the limitations of conventional antibiotic treatments due to the protective biofilm matrix, which hinders drug penetration and effectiveness. The use of TOB-LCNPs demonstrated a significant enhancement in antibiotic delivery and biofilm disruption, leading to improved bacterial eradication in vitro, as shown in **Figure 5**. The findings suggest that TOB-LCNPs represent a promising therapeutic strategy for managing chronic infections associated with cystic fibrosis.

Table 2 presents a selection of studies, including those described in the text and others, that use lipid-based nanomaterials for the treatment of bacterial infections.

3.2. Polymeric Nanomaterials

Polymeric nanoparticles (PNPs) are nano-sized particles (10–1000 nm) designed to encapsulate drugs within a polymeric matrix. These particles offer numerous possibilities for improved targeting of bacteria and biofilms, as well as for the development of responsive drug release systems, thanks to their simple design, ease of production, and the vast diversity of available polymers. PNPs have been extensively studied for drug stabilization and targeting.[90] Compared to free drugs, polymeric particles provide several advantages, including improved bioavailability, protection

Table 2. Lipid-based nanomaterials for the management of bacterial infections.

Vesicle type	Composition	Other components	Antimicrobial	Size [nm]	Infective agent	Notes	Refs.
Micelle	Amphiphilic NIR-Cy	–	Oritavancin	122.1 ± 10.4	*P. aeruginosa*	Theragnostic application	[76]
Liposome	DMPE, DPPC, Cholesterol	–	Tobramycin, N-Acetylcysteine	347.33 ± 62.27 229.47 ± 47.57	*E. coli, K. pneumoniae*, *A. baumannii*	MIC reduction	[77]
Liposome	Phosphatidyl choline, Cholesterol, p-dimethylamino pyridine	Oleic acid	Vancomycin	98.88 ± 1.92	*S. aureus* MRSA	pH responsive release	[67]
Liposome	Novel pH-sensitive lipids	–	Ampicillin	99.38 ± 6.59 105.60 ± 5.38	*S. aureus* MRSA	pH responsive release	[78]
Liposome	Lecithin	–	3T-CHO (photo sensibiliser)	≈191,7	*S. aureus* *P. aeruginosa*	Photodynamic therapy	[79]
Liposome	HSPC, DSPG, DSPE-PEG-OMe, Mannitol, sucrose, leucine	–	Ciprofloxacin	<4900	*P. aeruginosa*	–	[80]
Liposome	DSPE-PEG	FA	Moxifloxacin Oxi-αCD (ROS-responsive material)	254.2 ± 9.5	*P. aeruginosa*	ROS generation therapy	[81]
LNPs	Vitamin C lipid, DOPE, Cholesterol	–	mRNA codifying for AMP-Catenin B	127 ± 1	*S. aureus* *E. coli*	Survival improvement in MDR-bacteria-induced sepsis mice	[69]
SLNPs	glycerol palmitostearate, stearic acid	Poloxamer 188, Tween 80	Rifampin, Cis-2-Decenoic Acid	127.2 ± 2.8	*S. aureus* *S. epidermidis*	Enhanced antibiofilm activity	[82]
SLNPs	Precirol® ATO 5, oleic acid	Se	Ciprofloxacin	≈60	*S. aureus* *E. coli* *P. aeruginosa*	–	[83]
SLNPs	SA-3M	–	Vancomycin	132.9 ± 9.1	*S. aureus* MRSA	pH responsive	[74]
SLNPs	Glyceryl behenate, Tristerain, Precirol, Poloxamer 407	Tween 80, PVA, Poloxamer 407	QSI	<100	*P. aeruginosa*	Mucus penetration	[84]
SLNPs	SA, LA, OA	–	SA, LA, OA	<200	*S. aureus* *P. aeruginosa* *P. acnes*	Bacteria adhesion to surfaces was reduced	[85]
SLNPs	Palm oil, lecithin	Poloxamer, Tween 80	Doxycycline	≈300	*B. melitensis*	Intracellular infection treatment	[86]
SLNPs	Softisan 138, Softisan 154, Imwitor 900K, Dynasan 118	Stearic acid	Ciprofloxacin	165-320	*S. aureus* *E. coli* *P. aeruginosa*	Enhanced antimicrobial activity	[87]
NLC	Natural oil, myristic acid	Span 80	Quercetin	505.9 ± 31.8	*S. aureus*	Reduced cytotoxicity, enhanced drug diffusion in RHE model	[88]
NLC	lecithin, monostearin, soybean oil	PEG	Trimethoprim sulfamethoxazole	187 ± 9	MRSA	Improve the antibacterial effects of TMP/SMZ by 3 orders of magnitude	[89]
NLC	Monoolein, phytantriol	Pluronic F-127, propylene glycol	Glycoside hydrolase (PsIG), Tobramycin	≈190	*P. aeruginosa*	Two-stage release, antibiofilm activity	[75]

Abbreviations: Poly(ethylene glycol)−poly(ϵ-caprolactone) (PECL), Reactive oxygen species (ROS) trithiophene aldehyde (3T-CHO), Hydrogenated soybean phosphatidylcholine (HSPC), N- (methylpolyyoxyethylene oxycarbonyl)-1,2-distearoyl-sn-glycero-3-phosphoethanolamine (DSPE-PEG-OMe), Folic Acid (FA), Solid acid cleavable lipid (SA-M3), Poly(vinyl alcohol) (PVA), Stearic acid (SA), Lauric acid (LA), Oleic acid (OA), Reconstructed human epidermis (RHE).

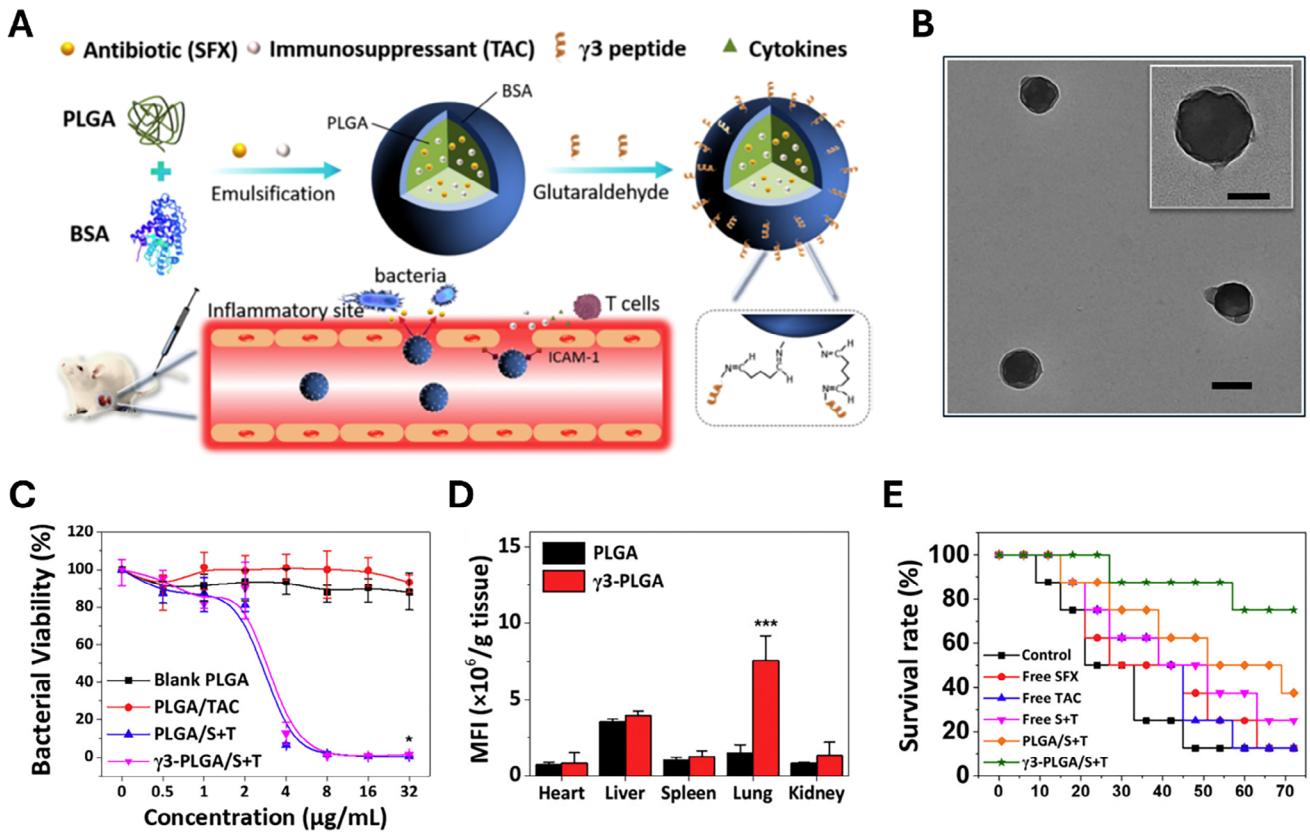

Figure 6. Inflammation-targeting polymeric nanoparticles deliver sparfloxacin and tacrolimus for combating acute lung sepsis. A) Schematic illustration of the nanoparticle synthesis process and selective targeting mediated by the γ3 peptide. B) Transmission electron microscopy (TEM) image showing the morphology of the nanoparticles. C) Antimicrobial activity against *P. aeruginosa* in vitro. D) Preferential accumulation of nanoparticles in inflamed tissues in a lung infection-induced sepsis animal model. E) Survival rate of different treatment groups ($n = 8$). Data are presented as mean ± SD ($n = 3$). $p < 0.05$ (*), $p < 0.01$ (**), $p < 0.001$ (***). Reproduced with permission.[94] Copyright 2020, Elsevier.

against enzymatic degradation, controlled release, and adaptability to different routes of administration.[91]

The physicochemical characteristics of PNPs are determined by the synthesis method followed and the polymers used in their formulation. These polymers can be categorized into two main groups: natural polymers (e.g., chitosan, gelatin, alginate, chondroitin sulfate) and synthetic polymers (e.g., poly(lactic-co-glycolic) acid (PLGA)) or poly(ϵ-caprolactone) (PCL), among others.[92] Polymer composition is considered the most critical factor influencing the in vivo release profile of antimicrobials. Several studies have reported the development of targeted and/or triggered delivery systems based on polymers and loaded with antibiotics for the treatment of infections.

The PNP category comprises a diverse range of nanostructures, each with unique architectures, properties, and applications. These include standard solid spherical NPs, as well as more specialized supramolecular forms such as dendrimers, polymersomes, polymeric micelles, and polyion complexes.

Standard solid polymeric NPs are typically composed of biodegradable polymers such as PLGA, PCL, poly lactic acid (PLA), poly glycolic acid (PGA), poly hydroxyl butyrate (PHB), polyester, poly dioxanone, among others. They possess a solid core that can encapsulate hydrophobic and hydrophilic drugs, offering a stable environment that protects therapeutic agents from degradation. Their surface properties can be modified to enhance cellular uptake and target specific bacterial species. These NPs facilitate sustained drug release, which is beneficial for treating biofilm infections over extended periods. They have been extensively validated, delivering various common antibiotics, as well as novel antimicrobials and antimicrobial nanomaterials.[93]

PLGA, an FDA-approved polymer in many drug delivery systems, is frequently selected for fabricating drug carriers due to its excellent biocompatibility and non-toxicity. It degrades into endogenous byproducts that can be safely metabolized by the body. By adjusting the ratio of PLA to PGA, the degradation rate of the particles—and consequently the drug release profile—can be controlled. PLGA particles can encapsulate hydrophobic antibiotics and, with appropriate surface coatings, remain stable in blood circulation. In a study by Yang et al., PLGA NPs were used to encapsulate sparfloxacin (SFX) and the immunosuppressant tacrolimus (TAC) to reduce excessive inflammatory responses from bacterial infections.[94] Additionally, the selective targeting γ3 peptide was conjugated to the surface of these loaded NPs, as illustrated in **Figure 6**.

This peptide binds selectively to the intercellular adhesion molecule 1 (ICAM-1), which is highly expressed on the surface of inflammatory endothelial cells. The developed platform demonstrated enhanced uptake by activated endothelial cells in vitro,

exhibiting strong antibacterial activity against both Gram-negative and Gram-positive bacteria. The targeting capability of γ3-PLGA NPs was further validated in a murine lung infection model, where γ3-modified NPs accumulated in the infected lungs five times more than unmodified ones. Additionally, mice treated with γ3-PLGA NPs released significantly lower levels of lactate dehydrogenase in bronchoalveolar lavage fluid compared to those treated with unmodified NPs. Lung histology confirmed that the modified NPs effectively reduced inflammation in infected lung tissue.

In the work of Yang et al., PLGA microspheres were also used to obtain an MRSA-responsive system mediated by an intrinsic enzymatic cascade in bacteria for the programmable release of antibiotics in an infected wound healing rat model.[95] Porous PLGA microparticles loaded with vancomycin were coated with fibrinogen and poly(L-lysine). The conversion of fibrinogen into fibrin, catalyzed by coagulases derived from MRSA, would facilitate the collapse of the integrity of the multilayered coating to release the loaded antibiotic. The system validated in vivo the triggered release of vancomycin mediated by the intrinsic enzymes of bacterial virulence factors. The size of MRSA-infected topical wounds was significantly reduced by nearly 100% after treatment for 12 days showing a 5-log decrease in the CFUs. The histological studies showed an increase in re-epithelization and tissue remodeling together with a 50% decrease in the levels of inflammatory factors.

3.2.1. Dendrimers

Dendrimers are highly organized polymeric macromolecules consisting of a core from which branch-like units grow outward. The term "dendrimer" does not refer to a specific chemical composition for a polymer but rather to a radially symmetrical branching molecular structure with three common elements: a nucleus, branches, and surface functional groups.[96] Dendrimers are effective drug delivery vectors due to their nanometric dimensions, low polydispersity, morphological uniformity, and large surface area-to-volume ratio, which enables them to carry therapeutic amounts of antimicrobials. Furthermore, some dendrimers have been reported to possess inherent antimicrobial activity.[97] The most commonly used polymers for dendrimer fabrication include poly(amidoamine) (PAMAM), poly(propylene imine) (PPI), and polyethylene glycol (PEG). As with other nanocomposites, the positive charge of the constituent polymers can give dendrimers innate targeting and biocidal capabilities by promoting the interaction with the negatively charged bacterial cell wall.[98] The amino or hydroxyl functional groups of these polymers provide opportunities to conjugate antimicrobials to them. For example, the amino groups of PAMAM can be conjugated to carboxyl groups in antibiotics such as vancomycin.[99] Notably, dendrimers can encapsulate hydrophobic drugs within their internal cavities and incorporate hydrophilic drugs into the functional groups near the surface. Antibiotics can also be incorporated as a structural part of the dendrimer,[100] as can antimicrobial peptides with proven efficacy against bacteria in both planktonic and biofilm states.[6] Lastly, dendrimers can be combined with other antimicrobial agents, such as silver or chitosan, to enhance their effectiveness.[101,102]

3.2.2. Polymersomes

Polymersomes are self-assembled nanostructures composed of amphiphilic block copolymers, resembling liposomes but with a more robust and stable polymeric membrane.[103] With a core-shell architecture, they enable the encapsulation of both hydrophilic drugs within their aqueous core and hydrophobic ones within their outer polymer layer.

In the study by Fenaroli et al., researchers demonstrated the effective targeting and intracellular delivery of antibiotics to infected macrophages both in vitro and in vivo using pH-sensitive nanoscopic polymersomes composed of Poly(2-methacryloyloxyethyl phosphorylcholine)–Poly[2-(dimethylamino)ethyl methacrylate] (PMPC–PDPA) block copolymers.[104] This study highlighted the ability of polymersomes to effectively target macrophages in vivo and colocalize with intracellular bacterial pathogens. The system significantly enhanced the efficacy of lysostaphin, vancomycin, gentamicin, and rifampicin against *Mycobacterium bovis*-BCG, *Mycobacterium tuberculosis*, and the well-established intracellular pathogen *S. aureus* Newman. Notably, the polymersomes also successfully penetrated Tuberculosis-like granuloma tissues—a notoriously challenging environment—in zebrafish models. This targeted delivery approach proved highly effective in eradicating multiple intracellular bacteria, including *M. tuberculosis*.

3.2.3. Polymeric Micelles

Polymeric micelles are formed from amphiphilic block copolymers that self-assemble into core-shell structures in aqueous environments.[105] The hydrophobic core can encapsulate hydrophobic drugs, while the hydrophilic shell stabilizes the micelles in solution. This configuration can enhance the solubility and bioavailability of poorly soluble antibiotics.[106] Polymeric micelles can respond to environmental stimuli (e.g., pH, temperature), allowing for controlled drug release in response to specific conditions within infected tissues. They have shown potential in targeting specific bacterial strains by modifying the surface properties with targeting ligands.[107]

In the study by Zhang et al., researchers developed polymeric micelles composed of a multifunctional pH-sensitive block copolymer (poly(ethylene glycol)-b-poly(β-amino ester)-b-poly(ethylene glycol)) grafted with a PEGylated lipid (biotin-PEG-b-PAE(-g-PEGb-DSPE)-b-PEG-biotin).[107] These micelles were loaded with ciprofloxacin and an anti-inflammatory agent, and subsequently coated with anti-mouse ICAM-1 antibodies. Given that ICAM-1 is highly expressed in infected microenvironments, as mentioned before, and correlates with increased vascular permeability, the antibody-coated micelles effectively targeted the activated vasculature in the infected tissues. Acidic and enzymatic cues triggered the disassembly of those polymeric micelles, facilitating drug release to clear bacteria and reduce inflammation. Biodistribution studies in mice infected with *P. aeruginosa* PA-103 revealed significant NPs accumulation in the lungs, confirming the targeting effectiveness of ICAM-1. In a separate experiment, *P. aeruginosa* was directly administered to the lungs, followed by the NP administration 4 h later. Analysis of bronchoalveolar lavage fluids demonstrated a remarkable inhibition

of bacterial proliferation compared to equivalent doses of free ciprofloxacin, along with a mitigation of the inflammatory response. Notably, a survival rate of 90% was observed in mice administered a lethal dose of bacteria, mimicking sepsis conditions.

In the same line, Wang et al., developed a novel strategy to enhance the treatment of pulmonary bacterial infections by utilizing folic acid-conjugated PEG to coat NPs formed from phenylboronic ester-modified cyclodextrin that encapsulates moxifloxacin.[81] This approach aimed to improve the targeting of macrophages and to facilitate penetration through the mucus often present in lung infections. In their study, the biodistribution of these NPs was analyzed in a mouse model of pulmonary infection caused by various clinical isolates of *P. aeruginosa* using in vivo imaging. Their results showed that the NPs had longer retention times in lung tissues compared to free moxifloxacin, with the fluorescence of the polymeric micelles detected 24 h post-injection. The accumulation of the particles in infected lung tissues was attributed to the overexpression of folic acid receptors on the surfaces of activated macrophages at inflammation sites. Furthermore, the PEGylated micelles demonstrated efficient mucus penetration, arguably due to the hydrophilic properties of PEG. Notably, the survival curve for the infected mice revealed a 40% survival rate for those treated with the NPs, in contrast to only 20% for those treated with equivalent doses of free moxifloxacin.

Lastly, Cheng et al. developed a drug delivery system utilizing PCL, a biocompatible and bioresorbable polyester that biodegrades through hydrolysis of its ester linkages into non-acidic products, making it suitable for long-term drug delivery.[108] PCL can be disrupted by bacterial lipase, which facilitates the release of loaded antibiotics into the bacterial environment. To achieve on-demand release at infection sites, they designed antibiotic-loaded polymeric micelles that respond to both lipase and varied pH levels. They synthesized lipase-sensitive PCL through ring-opening polymerization initiated by PEG and conjugated vancomycin via a pH-cleavable hydrazine bond, encapsulating ciprofloxacin in the core of the resulting micelles. This system effectively accumulated at infection sites due to the enhanced permeation and retention effect while selectively targeting bacteria thanks to the vancomycin. Under acidic conditions, the vancomycin shell was cleaved, and the PCL core degraded in the presence of lipase, allowing for the release of ciprofloxacin. In vivo studies using a murine model of *P. aeruginosa* PAO1 infection demonstrated a significant decrease in lethality, with the survival rate increasing from 14% after one dose to 43% and 83% after two and three doses, respectively.

3.2.4. Polyion Complexes

Polyion complexes (PICs) are formed through the electrostatic interactions between oppositely charged polyelectrolytes, resulting in a nanoscale structure that can encapsulate therapeutic agents.[109] These complexes are particularly useful for delivering nucleic acids, such as siRNA, as they protect genetic material from degradation and facilitate cellular uptake. In the context of bacterial infections, polyion complexes can be engineered to deliver antimicrobial agents or genetic therapies that target bacterial resistance mechanisms. Additionally, cationic polymers can exhibit inherent bactericidal activity due to their electrostatic interactions with the negatively charged bacterial cell wall. This interaction disrupts the integrity of the bacterial membrane, leading to cell lysis and death, further enhancing their potential as effective antimicrobial agents.

Wei et al., investigated the bactericidal properties of cationic polymers poly[3-(acrylamido)propyl]trimethylammonium chloride (PAMPTMA) and PAMPTMA-b-poly(butyl methacrylate) when formulated with anionic surfactants, discovering their superior fast-bactericidal activity against the Gram-negative bacterium *E. coli* ATCC 8739.[110] Their results showed an impressive 99.99% killing rate within just 10 min of treatment, significantly outperforming either the cationic polymer or the anionic surfactant alone, both of which lacked bactericidal efficacy in such a short time frame. This finding contradicts previous studies that suggested that cationic polymers lose their activity due to fouling by anionic surfactants. Instead, the authors explained that the formation of PICs concentrates positive charges, allowing them to attach to the negatively charged bacterial surfaces. This interaction leads to a high local concentration of positive charges, which rapidly permeabilizes both the outer and inner membranes of bacteria, resulting in a swift cell death. The successful demonstration of the fast-bactericidal activity of PICs against Gram-negative bacteria opens numerous potential applications in commercial formulations, especially in consumer products where alternative antibacterial agents are urgently needed. Furthermore, this novel approach to rapid chemical antisepsis using surfactant formulations could be particularly beneficial in clinical settings, where, as it was mentioned before, the presence of AMR pathogens is a growing concern.

In the same lines, Insua et al., focused on the preparation and characterization of PICs containing the last-resort antimicrobial polymyxin B (Pol-B).[111] They synthesized these particles using poly(styrene sulphonate) (PSS) as an inert component, exploring a range of degrees of polymerization to evaluate how the multivalency of this electrolyte affects both the stability and antimicrobial activity of the derived particles. Their findings revealed that while PICs formulated with longer polyelectrolytes demonstrated greater stability under simulated physiological conditions, those created with shorter polyelectrolytes exhibited enhanced antimicrobial activity. By tailoring the degree of polymerization and the component ratios, the researchers identified a formulation that sustained an inhibitory effect on the growth of *P. aeruginosa* PAO1V, achieving over 10 000 times greater efficacy in reducing viable colonies compared to their previously reported formulation.

Table 3 presents a selection of studies, including those described in the text and others, that use polymeric nanomaterials for the treatment of bacterial infections.

3.3. Metal-Based Materials

3.3.1. Metallic Nanoparticles

Metal nanoparticles (MNPs) are arguably the most popular nanomaterials for antimicrobial applications. Their multimodal bactericidal capacity, straightforward synthesis, functionalization potential, plasmonic characteristics, small size, high

Table 3. Polymeric nanomaterials for the management of bacterial infections.

Particle type	Composition	Other components	Antimicrobial	Size [nm]	Bacteria	Notes	Refs.
PNP	PLGA	DOTAP	Vancomycin	207.83 ± 2.06	MRSA	Enhanced antibiofilm activity	[112]
PNP	Gelatin	–	Vancomycin	97.3 ± 3.4	*S. aureus* *E. coli* *S. epidermidis* *P. vulgaris* *S. marcescens* *P. aeruginosa*	–	[113]
PNP	Chitosan	–	Ruthenium dioxide nanosheets, $[Ru(bpy)_2(\cdot tip)]2+$	≈140	*P. aeruginosa*	Photothermal therapy, ROS generation therapy	[114]
PNP	Chitosan	–	Ciprofloxacin, ceftriaxone, gentamicin	180 ± 20	*S. Typhimurium*	Intracellular infection treatment	[115]
PNP	Chitosan	BSA	ε-poly-l-lysine	223 ± 1.7	*H. pylori*	Bacterial biofilm eradication	[116]
PNP	Alginate	Sodium Caseinate	Nisin (AMP)	192	*E. faecium*, *S.epidermidis* *E. faecalis*	pH responsive release	[117]
PNP	PCL	–	Cefotaxime	216	*S. aureus* *E. coli*	–	[118]
PNP	PLGA	Chitosan	Moxifloxacin, amikacin	312 – 640	*M. tuberculosis*	Intracellular infection treatment	[119]
PNP	PLGA	–	Gentamycin	1500 – 2400	*E. coli*	–	[120]
Dendrimer	PAMAM	–	Ag+	≈5.4	*S. aureus* *P. aeruginosa* *E. coli*	Enhanced antimicrobial activity	[101]
Dendrimer	PGLD	Chitosan	Boron	–	*S. aureus* *P. aeruginosa*	–	[102]
Dendrimer	PAMAM	–	Vancomycin	–	*S. aureus* MRSA *P. aeruginosa* *E. coli* *K. pneumonia* *S. typhimurium*	Enhanced Gram-negative susceptibility against vancomycin	[121]
Dendrimer	PAMAM	Oleylamine, Kolliphor RH40	Vancomycin	173.9 – 252.7	MRSA	pH responsive release	[122]
Dendrimer	PAMAM	Chitosan	Methicillin, NO	–	*E. coli* MRSA	Synergistic antibacterial activity	[123]
Dendrimer	PEG	–	Cefazolin	≈15	*S. aureus* *E. coli* *S. epidermidis* *S. pneumoniae* *P. mirabilis* *H. influenziae*	ROS generation therapy	[124]
Polymersome	PMPC–PDPA copolymers	Cy5	Lysostaphin, vancomycin, gentamicin, rifampicin, isoniazid	≈100	*S. aureus* BCG *M. marinum* *M. tuberculosis*	pH responsive, Tuberculosis-like granuloma tissues penetration	[104]
Polymersome	Hyaluronic acid	Oleylamine	Vancomycin	248.7 ± 3.08	MRSA	–	[125]
Polymeric micelle	Cationic and non-ionic triblock copolymers	Pluronic F127	Ciprofloxacin	34.6 – 37.1	*S. aureus*	Prolonged release, antibiofilm activity	[106]
Polymeric micelle	DSPE-PEG, Lecithin	Folic acid	ROS-responsive material (Oxi-αCD), moxifloxacin	254.2 ± 9.5 – 266.2 ± 1.0	*P. aeruginosa*	Lung accumulation, mucus penetration, enhanced antimicrobial activity in vivo	[81]
Polymeric micelle	DSPE-PEG, PAE	Biotinylated anti-ICAM1 antibody, avidin	Ciprofloxacin	450 ± 100	*P. aeruginosa*	pH/lipase responsive	[107]

(*Continued*)

Table 3. (Continued)

Particle type	Composition	Other components	Antimicrobial	Size [nm]	Bacteria	Notes	Refs.
Polymeric micelle	PCL-PEG	–	Vancomycin, ciprofloxacin	77	*P. aeruginosa*	pH/Lipase responsive	[108]
Polyion complex	Cationic polymer (PAMPTMA), anionic surfactant (SDBS)	–	PAMPTMA	≈70	*E. coli*	Fast bacterial killing	[110]
Polyion complex	Branched PEI, anionic peptide	–	PEI	127 ± 42	*P. aeruginosa*	Elastase enzyme-responsive, reduced toxicity	[126]

Abbreviations: Polyethyleneimine (PEI), Polyglycerol with dendritic structure (PGLD)

surface-to-volume ratio, and capacity to bind within bacterial cells, contribute to their effectiveness as potent antimicrobial agents.[127] MNPs, primarily composed of Au, Ag, or Cu, exhibit strong antimicrobial activity, although they possess potential toxicity to mammalian cells.[128] However, the integration of MNPs into biological or organic systems with reduced toxicity has opened a wide range of applications in biomedical research.

MNPs display innate antimicrobial activity that can overcome common bacterial resistance mechanisms, such as target modification, overexpression of efflux pumps, enzymatic inactivation, and others.[129] The bactericidal mechanisms of NPs include: 1) agglomeration of NPs on the cell wall and membrane, altering their structural integrity, 2) generation of reactive oxygen species, 3) inhibition of protein and nucleic acid synthesis, and 4) inhibition of biofilm formation.[17,130] It is unlikely that resistance to NPs will develop, as their targets and modes of action are multiple, although some resistance mechanisms have been reported.[131,132] NPs such as Ag or Au have been shown to be effective against both Gram-positive and Gram-negative bacteria, either alone or in conjunction with antibiotics,[133,134] and have garnered considerable attention. Au NPs exhibit powerful antibacterial effects through multiple mechanisms. They disrupt bacterial integrity by creating pores in the cell wall, leading to leakage of cellular content and eventual cell death. Additionally, Au NPs can bind to bacterial DNA, inhibiting transcription and halting bacterial replication. Owing to their low cytotoxicity against eukaryotic cells, stable storage, and easy surface functionalization, gold NPs have been extensively applied as drug delivery carriers.

Importantly, Au NPs possess unique optical properties. Under visible (VIS) or near-infrared (NIR) irradiation, depending on their structure and size, Au NPs generate photothermal heat, which can be harnessed to trigger the release of drugs. Liu et al. developed a chemo-photothermal platform using gold nanorods (GNRs) coated with polydopamine (PDA) and further functionalized with glycol chitosan (GCS) for improved biocompatibility.[135] This system was loaded with silver ions (Ag^+), creating an antimicrobial depot (Ag^+-GCS-PDA@GNRs). The PDA's catechol groups chelate the silver ions, enhancing their antimicrobial effects, while the glycol chitosan and Ag^+ provide pH-sensitive release and infection-specific targeting capabilities, as shown in **Figure 7**. Glycol chitosan was selected because it shows charge reversal properties depending on the pH showing less than 10% Ag^+ release at pH 7.4 after 8 h whereas at pH 6.3 more than 21% of antimicrobial Ag^+ was detected in only 1 h.

This composite material was tested in a murine model having subcutaneous bacterial abscesses. The system showed strong site-specific accumulation, aided by electrostatic interactions between Ag^+ ions and negatively charged bacterial cells. Upon NIR irradiation, the infected area's temperature rose to 50 °C, demonstrating effective photothermal action for bacterial eradication. This chemo-photothermal approach produced potent in vivo bactericidal effects, confirming the synergy between photothermal therapy and the antimicrobial action of the silver-loaded nanorods.

Silver NPs are the most extensively used material due to their excellent antimicrobial properties based on the ability to release Ag^+ ions, which can interact with thiol groups in enzymes and proteins that support bacterial life, thus reducing viability.[136] However, Ag NPs easily aggregate, and after ion release, the NP cores are hard to recover and may accumulate in tissue, causing adverse effects. Consequently, Ag should be combined with polymers to obtain less cytotoxic biomimetic biomaterials.[137] In this previous work, a hydrogel combining Ag and gentamicin was prepared for efficient synergistic bacteria eradication, overcoming AMR through different antibacterial mechanisms. Hyaluronic acid was grafted into 3-aminophenylboronic acid to create nanocarriers containing both Ag^+ and gentamicin. These nanocarriers were incorporated into a chitin-based hydrogel to be used as a disinfectant coating material. Ag^+ and gentamicin were simultaneously released at the inflammation site under bacterial acidic conditions and the presence of hyaluronidase. A dorsal wound infection model in rats was used to evaluate the therapeutic efficacy in terms of antibacterial activity and wound healing. The system containing Ag and gentamicin demonstrated a superior ability to effectively prevent wound infection and significantly accelerate wound healing.

In this context, the combination of MNPs with antibiotics has been studied to revive the effectiveness of antibiotics against multi-resistant strains. MNPs can serve as physical carriers, transporting antibiotics directly to the bacteria, thereby increasing bactericidal activity. This enhancement is primarily due to the affinity of NPs for the bacterial cell wall, causing a localized increase in antibiotic concentration.[138] MNPs are typically

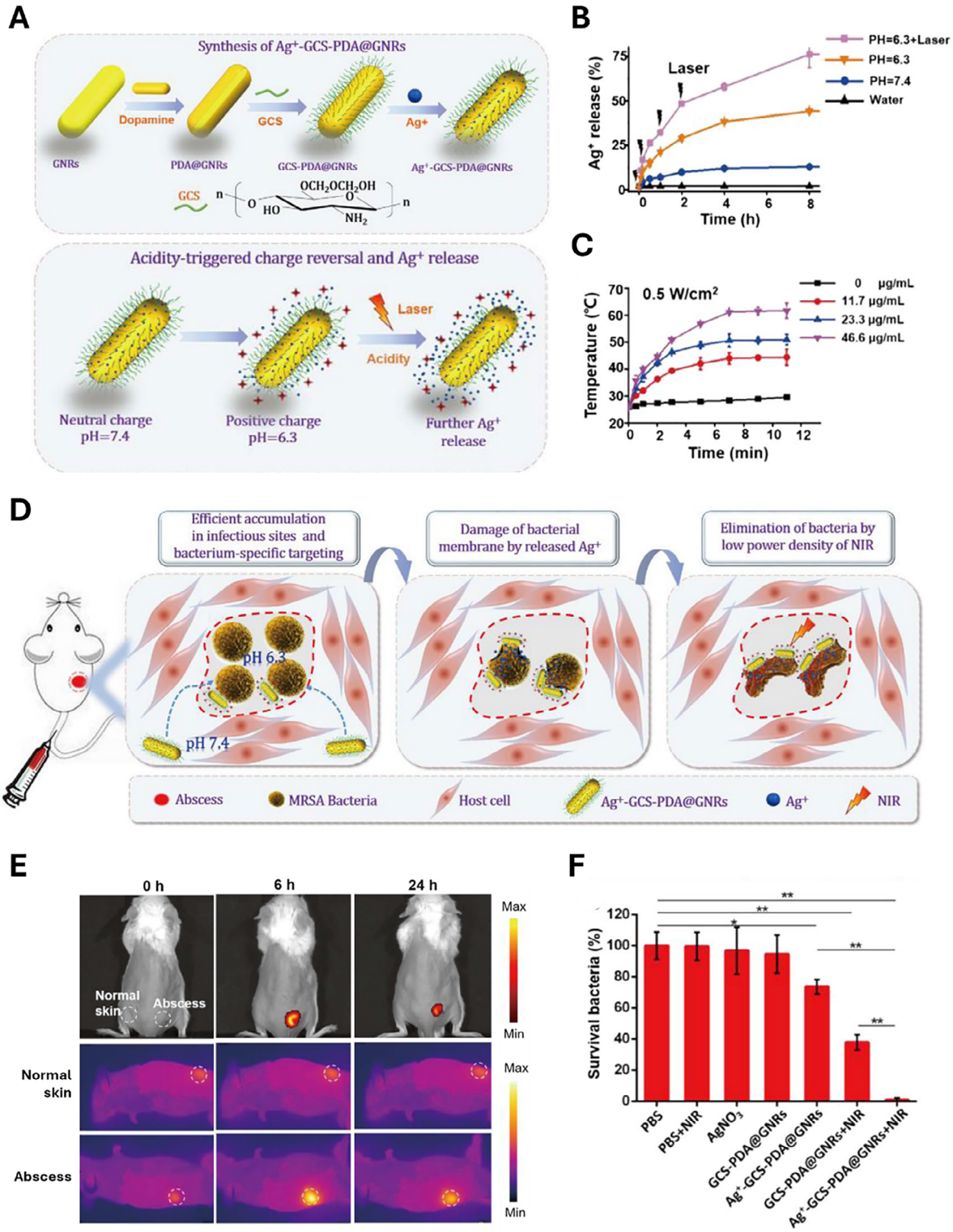

Figure 7. Gold nanorods-based infectious site-targeted chemo-photothermal therapy. A) Schematic illustration of the synthesis of Ag^+-GCS-PDA@GNRs, the acidity-triggered charge reversal and Ag^+ ion release mechanism. B) Release profile of Ag^+ ions from Ag^+-GCS-PDA@GNRs in media at pH 7.4 and 6.3, with or without NIR laser irradiation. C) Temperature evolution of PBS buffer and Ag^+-GCS-PDA@GNRs suspensions at varying concentrations (pH 6.3) under 808 nm NIR laser irradiation (0.5 W/cm^2). D) In vivo bacteria-specific targeting and combined chemo-photothermal therapeutic effects. E) NIR fluorescence and thermal imaging of abscess-bearing mice intravenously injected with Ag^+-GCS-PDA@GNRs (4.7 mg k^{-1} g) at 0, 6, and 24 h post-injection. F) Quantification of MRSA bacterial CFUs under different treatment conditions. $p < 0.05$ (*), $p < 0.01$ (**), $p < 0.001$ (***). Reproduced with permission.[135] Copyright 2018, Springer Nature.

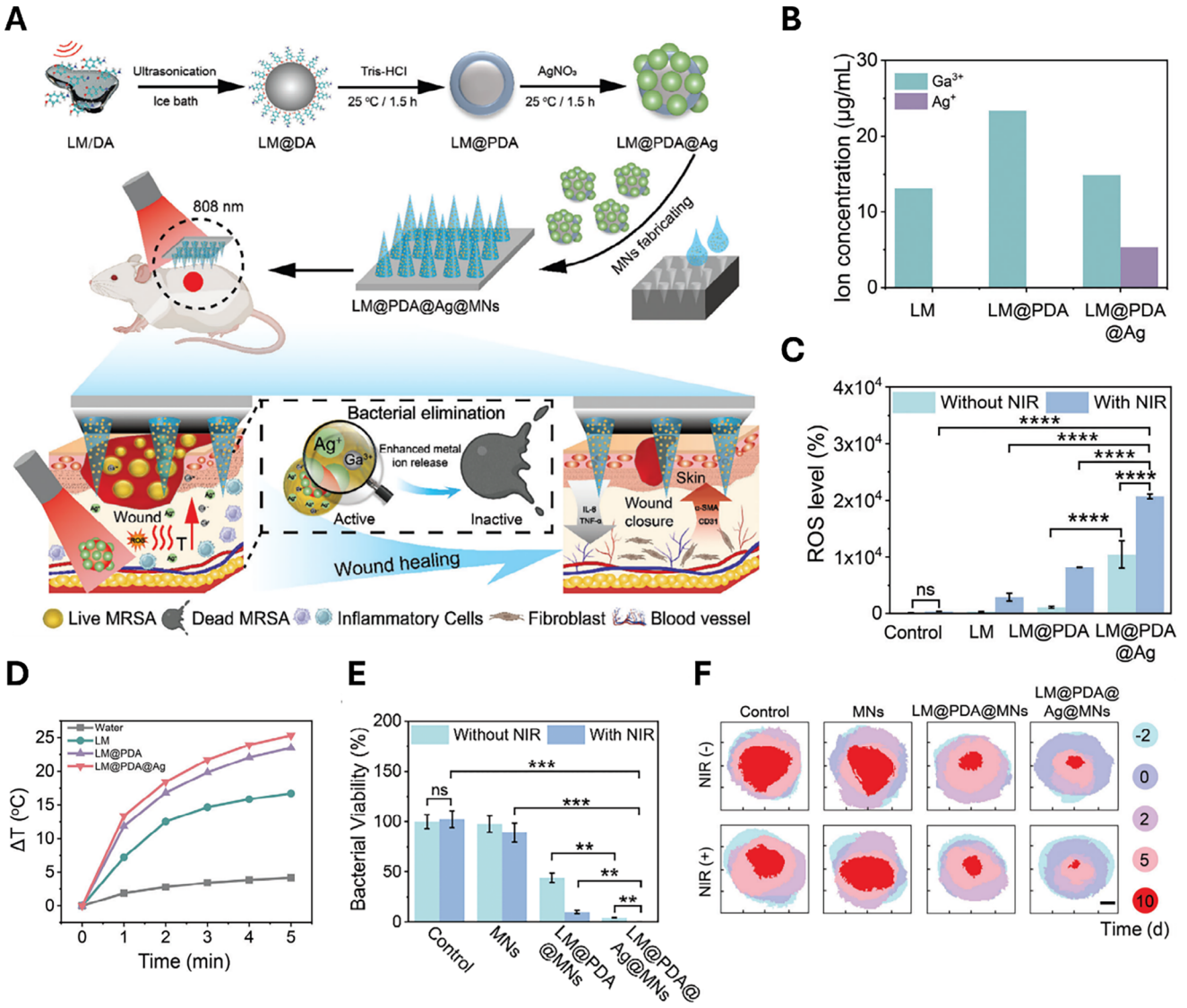

Figure 8. LM@PDA@Ag microneedle patches for NIR-enhanced treatment of MRSA-infected wounds. A) Schematic illustration of the synthesis and application of LM@PDA@Ag microneedle patches. The fabrication involves PDA modification of gallium-based liquid metal nanoparticles, followed by in situ silver nanoparticle formation and integration into microneedle patches. Upon NIR laser irradiation, the system promotes metal ion release, ROS generation, and photothermal antibacterial activity. B) Metal ion release profiles from LM, LM@PDA, and LM@PDA@Ag nanoparticles. C) Quantification of ROS levels in MRSA after incubation with various nanoparticles, with or without NIR irradiation. D) Temperature elevation of LM@PDA@Ag nanoparticle suspension (0.5 mg/mL) under 808 nm NIR laser irradiation (0.7 W/cm^2, 5 min). E) Relative survival rate of MRSA after different nanoparticle treatments with or without NIR irradiation, based on in vitro CFU counts. F) Contour maps showing dynamic wound healing progression in a murine model of topically infected wounds. $p < 0.05$ (*), $p < 0.01$ (**), $p < 0.001$ (***). Reproduced with permission.[142] Copyright 2024, Wiley.

synthesized by chemical reduction from an inorganic salt. The conjugation of antimicrobials to metal NPs generally occurs in two ways: via adsorption mediated by intermolecular forces such as charge differences or through covalent bonding.[139]

The application of nanomaterials extends to surface modifications, which are particularly relevant in the context of implants. Thanks to their biocompatibility and mechanical properties, titanium and titanium alloys are widely used in orthopedic implants. However, these implants face the serious problem of surface colonization by pathogens, which leads to biofilm formation. Once established, biofilms are extremely challenging to treat clinically. Although modifying material surfaces can reduce bacterial adhesion, surfaces that prevent bacterial adherence often also inhibit cell adhesion, which can hinder bone tissue formation.[140] In this context, Yuan et al. developed a Ti-based material with both anti-infective properties and efficient osseointegration. TiO_2 nanotubes were fabricated on titanium foils to serve as vancomycin reservoirs.[141] Then, multilayer chitosan-catechol and sodium hyaluronate-catechol films were deposited on the modified surfaces. The sodium hyaluronate layer degrades in the presence of hyaluronidase secreted by bacteria, triggering the release of antibiotics that can target both adherent and planktonic

bacteria. Additionally, catechol groups promote primary osteoblast adhesion by specifically upregulating the gene expression of integrin $\alpha v\beta 3$. The antibacterial properties and osseointegration of the Ti-based materials were tested in a murine model. Different implants were inserted into the femoral medullary cavities of rats, which were subsequently infected with *S. aureus*. After one month of implantation, no clustered bacteria were found; however, several bone-related cells had adhered and mineralized on the substrates.

Lastly, Wang et al. developed a gallium-based nanostructure designed to act as an antibacterial metal ion reservoir, offering a highly effective strategy for eliminating MRSA infections.[142] Their approach involved synthesizing gallium nanoparticles through a two-step process followed by polydopamine (PDA) modification, which played a dual role: facilitating Ga oxidation to generate a high-valence Ga-enriched surface for enhanced metal ion release and enabling the in situ formation of Ag nanoparticles to further enhance bactericidal activity. This liquid metal Ga-based nanostructure (LM@PDA@Ag) exhibited synergistic effects, including increased metal ion release, ROS generation, and photothermal antibacterial activity under NIR laser irradiation. The combination of these mechanisms led to bacterial membrane disintegration and nearly 100% MRSA eradication in vitro. To ensure precise and efficient delivery to infected tissues, LM@PDA@Ag NPs were incorporated into a PVA-based microneedle patch (LM@PDA@Ag@MNs), allowing for deep skin penetration, localized metal ion release, and sustained antibacterial effects, as shown in **Figure 8**.

In vivo studies demonstrated that this microneedle-based therapy not only achieved effective bacterial elimination and inflammation reduction but also stimulated collagen deposition, blood vessel formation, and tissue regeneration, ultimately accelerating wound healing. This study introduces, for the first time, a Ga-enabled nanostructure as a targeted metal ion reservoir, providing a promising nanoplatform for the treatment of MDR bacterial infections and advanced tissue regeneration strategies.

3.3.2. Metal–Organic Frameworks

Metal-organic frameworks (MOFs) are crystalline materials composed of transition metal ions bound to organic ligands through coordination bonds, hydrogen bonds, or electrostatic interactions.[143] The characteristics of MOFs include high porosity, large surface area, high carrier capacity, variability, and biodegradability.[144] Among these, porosity makes MOFs excellent candidates for functioning as carriers and platforms for the sustained release of antimicrobials.[145] Their well-defined structures allow them to encapsulate molecules of various sizes, ranging from small molecules to larger ones like DNA or proteins.[146–148] These molecules can bind to MOFs either covalently or non-covalently. Depending on the MOF composition, the release of the entrapped compounds can be triggered by external stimuli such as pH, light, temperature, etc.[149] For example, the interactions that hold the drug encapsulated inside an MOF can be pH-dependent, as in the case of MOF ZIF-8. Under neutral pH conditions, the release of drugs within the MOF is minimal, whereas rapid release occurs when the medium is acidified.[150]

MOFs can exhibit antimicrobial activity on their own due to their composition. When MOFs degrade in a physiological environment, the metals functioning as nodes (e.g., Ag, Au, Zr, Se) can be released as free ions, exerting bactericidal effects.[151] As an example, the bactericidal activity of Ag ions has also been combined with MOFs to develop an on-demand nanoplatform for the effective treatment of wounds infected with MRSA.[152] Moreover, the ligands within MOFs may have bactericidal properties as well. These features can complement the antimicrobial drug cargo and work synergistically, enhancing their overall antimicrobial effectiveness.[153,154] The surface of MOFs can also be easily modified to provide targeting capabilities. Additionally, various polymers have been used as capping agents to increase the circulation time of MOFs, prevent their degradation, and regulate the release of their cargo.[155] Sun et al. developed Cu/Zn bimetallic MOFs on MnS nanoparticles encapsulating prodrugs (i.e., amidine-containing azide and alkyne) and coated with hyaluronic acid.[156] In response to the hyaluronidase produced by pathogenic bacteria and the acidic biofilm pH, the nanoparticles degraded to release the prodrug and expose the MnS, which triggered the catalytic production of ROS. The decomposition by-products of MnS (i.e., H_2S) triggered a biorthogonal reaction to convert the prodrug into the active antibacterial drug (a bisamidine analog). The nanoparticulated system showed a superior biofilm reduction in vivo in an implant-related periprosthetic infection model.

Table 4 presents a selection of studies, including those described in the text and others, that use metal-based nanomaterials for the treatment of bacterial infections.

3.4. Other Inorganic Materials

3.4.1. Carbon Based Nanomaterials

Carbon-based nanomaterials (CBNs) are emerging as versatile platforms for treating bacterial infections, including structures like carbon nanotubes (CNTs), graphene-based materials, and carbon dots (CDs). These nanomaterials offer distinct advantages due to their large surface areas, tunable surface chemistry, and diverse antibacterial mechanisms. For instance, CNTs functionalized with antibiotics, such as amphotericin B, have shown effectiveness against both fungal and bacterial infections, suggesting potential across a broad range of antimicrobial applications.[155] The needle-like structure of CNTs enables them to penetrate bacterial membranes, causing cytoplasmic membrane disruption, leakage of cellular contents, and ultimately cell death. This direct contact mechanism has demonstrated efficacy against both Gram-positive and Gram-negative bacteria.[172]

Graphene-based materials also show promise for controlled drug release. For example, graphene oxide (GO) can be loaded with antibiotics like gentamicin and ciprofloxacin to enhance drug stability and enable pH-sensitive or enzyme-sensitive release.[173,174] Additionally, graphene's oxidative properties contribute to antibacterial effects by causing membrane damage and lipid peroxidation, leading to further bacterial cell disruption.[175,176] This combination of disruptive action and functionalization potential makes CBNs a powerful tool in antimicrobial applications, particularly for addressing biofilms and drug-resistant pathogens.

Table 4. Metal-based nanomaterials for the management of bacterial infections.

Material	Composition	Other components	Antimicrobial	Size [nm]	Bacteria	Effect	Refs.
Metallic NPs	Au rods	PDA, Glycol Chitosan	Ag+	68 ± 2 long, 21 ± 1 wide	MRSA	Chemo-thermal focal infection therapy	[135]
Metallic NPs	Au	–	Ciprofloxacin	≈24	*E. faecalis*	Bacteria eradication in vivo	[157]
Metallic NPs	Au	–	Virstatin	≈17	*V. cholerae*	Enhanced bactericidal activity, toxin production reduction	[158]
Metallic NPs	Au		Vancomycin	≈5	*E. coli* *E. faecium* *E. faaecalis*	Enhanced bacterial activity	[159]
Metallic NPs	Ag	Hyaluronic acid	Ag+, tannic acid, gentamicin	10–30	*E. coli* *S. aureus* MRSA	Enzyme-responsive chemotherapy	[137]
Metallic NPs	Ag	–	Cephradine, Vildagliptin	≈85,33	*E. coli* MRSA *P. aeruginosa* *K. pneumoniae, B. cereus* *S. pyogenes*	Enhanced bacterial activity against resistant bacteria	[160]
Metallic NPs	Ag	–	Vancomycin	86 ± 4.5	*E. coli* *S. aureus*	Enhanced bactericidal activity	[161]
Metallic NPs	Cu	Maltol	Ciprofloxacin, streptomycin	50 – 60	*E. coli* *P. aeruginosa* *K. pneumoniae*, *P. mirabilis*, *K. oxytoca*	Synergistic effect	[162]
Metallic NPs	Cu	HPG	Tetracycline	65	*S. aureus*	Enhanced bactericidal activity	[163]
Metallic NPs	Ga, Ag	PDA	–	≈600	MRSA	Chemotherapy ROS generation Phototermal theraphy	[142]
Metallic NPs	Se	Ru complexes	UBI29-41 (AMP)	78 ± 13	*S. aureus* *E. coli*	Theragnostic application	[164]
Metallic NPs	Se	Ascorbic acid	Lysozyme	71 – 84	*S. aureus* *E. coli*	Synergistic effect	[165]
Metallic NPs	ZnO	–	Ciprofloxacin	20 – 26	*E. coli* *Klebsiela spp.* *B. subtilis* *Streptococcus spp.*	Synergistic effect	[166]
Metallic surface	Ti	Chitosan, Hyaluronic acid, catechol	Vancomycin	≈70	*S. aureus*	Enzymatic triggered release	[141]
MOF	Ag-MOF	Platelet membrane coating	Vancomycin	≈148	*S. aureus* *E. coli* *P. aeruginosa* MRSA	Platelet reduces clearance of RES	[167]
MOF	ZIF-8	PDA coating	Vancomycin	175.9 ± 2.74	*S. aureus* *E. coli*	Photothermal therapy. pH triggered release	[168]
MOF	ZIF-8	–	Gentamycin	200	*S. aureus* *E. coli*	pH triggered release	[169]
MOF	MIL-53	Chitosan coating	Vancomycin	586.54 ± 34.24	*S. aureus*	Enhanced bactericidal activity	[155]
MOF	MIL-100	–	Amoxicillin, potassium clavulanate	273 ± 23	*S. aureus*	Intracellular infection treatment	[147]

(*Continued*)

Table 4. (Continued)

Material	Composition	Other components	Antimicrobial	Size [nm]	Bacteria	Effect	Refs.
MOF	MIL-100	3-azido-d-alanine loading, Pluronic F-127 polymer	US-TPETM – dibenzo cyclooctyne NPs	≈120	MRSA	Photodynamic therapy and imaging	[170]
MOF	PCN-224 (MOF)	Hyaluronic acid	Ag+	≈85	*E. coli* MRSA	ROS generation therapy	[171]
MOF	Cu/Zn bimetallic MOFs on MnS nanoparti-cles	Hyaluronic acid	Cu-click reaction on prodrugs to produce bisamidine analoges	≈340	*S. aureus*	ROS generation and superior antibiofilm effects	[156]

Abbreviations: Hyperbranched polyglycerol (HPG), reticuloendothelial system (RES), Zeolitic Imidazole Framework-8 (ZIF-8), *Matériaux de l'Institut Lavoisier*-53 (MIL-53), *Matériaux de l'Institut Lavoisier*-100 (MIL-100), ultrasmall 2-(1-(5-(4-(1,2,2-tris(4-methoxyphenyl) vinyl) phenyl) thiophen- 2-yl) ethylidene) malononitrile (US-TPETM).

Carbon dots are especially promising for bacterial imaging, detection, and inactivation, although their role as antibiotic carriers is still relatively scarce. Functionalized with antibiotics, CDs can selectively target and inactivate pathogens,[177] and their ability to generate ROS under light irradiation adds a photodynamic antibacterial capability.[178] Furthermore, CBNs effects can be enhanced by incorporating MNPs or heteroatoms, which introduce photothermal or photodynamic effects to intensify bacterial inactivation under specific light conditions.[179]

In the study by Ji et al., a composite nanomaterial combining graphene nanosheets (GS), mesoporous silica and hyaluronic acid was developed to combat drug-resistant biofilm infections.[180] The graphene nanosheets enhanced pore volume for effective drug loading and enabled photothermal therapy. These researchers created a hyaluronidase-sensitive composite that incorporated ascorbic acid (AA), a prodrug of hydrogen peroxide (H_2O_2), within a matrix of graphene and mesoporous silica conjugated with hyaluronic acid-dopamine (AA@GS@HA-MNPs). Upon reaching the infection site, the hyaluronic acid-dopamine conjugate was degraded by hyaluronidase, an enzyme secreted by bacteria in infectious environments, releasing ascorbic acid, which was converted into hydroxyl radicals that disrupt bacterial cell membranes. A scheme of these mechanisms is depicted in **Figure 9**.

In vivo evaluations using those AA@GS@HA-MNPs and conducted using an implant-related periprosthetic infection model, revealed that the treated area exhibited a notable trend toward healing. This outcome suggests that the developed "on-demand" nanocarrier effectively targets the infection site, releasing its therapeutic payload to disperse biofilms and inactivate embedded bacteria.

In the same line, Sun et al. explored the properties of carbon nitride, which has a relatively narrow band gap and strong reduction ability, enabling it to respond to both UV and VIS light.[23] Upon irradiation, the generated electrons activate electron acceptors, such as O_2 molecules, leading to the production of reactive radicals, such as singlet oxygen and hydroxyl radicals. Carbon nitride serves not only as an efficient water-splitting agent but also as a promising nanophotosensitizer, characterized by its stability, nontoxicity, biocompatibility, and high quantum yield. This reported research also highlighted the importance of QS in bacterial behavior, noting that various phenotypes controlled by QS facilitate invasion of host cells and contribute to the formation of drug-resistant biofilms. In their study, they utilized hollow carbon nitride nanospheres (HCNS) to encapsulate luteolin, a QS inhibitor, alongside with the antibiotic ampicillin to create a synergistic antibiofilm system, as depicted in **Figure 10**.

The developed nanospheres were further capped with hyaluronic acid to enhance their response to bacterial infective microenvironments. As described in previous systems, hyaluronic acid is degraded by bacterial hyaluronidase, resulting in a two-step release of the encapsulated drugs. In the initial stage, luteolin was released from the shell of the spheres, effectively modulating the QS of MRSA to inhibit biofilm formation, thereby enhancing the subsequent antibiotic action released in the second stage. Under irradiation, the nanospheres generated ROS, contributing to bacterial damage and biofilm destruction. The efficacy of this antibiofilm nanosystem was evaluated in a murine model of implant-related periprosthetic infection, where catheters were pre-colonized with MRSA demonstrated significant swelling and purulence, having the tissues of the treated animals showing reduced cell debris and a clear regeneration of their epidermis.

3.4.2. Mesoporous Silica Nanomaterials

Mesoporous silica nanoparticles (MSNs) have been shown to be effective nanocarriers for stimuli-responsive and controlled drug delivery, with a wide range of applications.[181] These materials exhibit a tunable and narrow pore size distribution (2–30 nm), adjustable pore structures, high specific surface areas (up to 1500 $cm^2\ g^{-1}$), and high pore volumes (≈1 $cm^3\ g^{-1}$), as well as inertness and robustness.[182,183] Additionally, they demonstrate thermal and chemical stability, biocompatibility, and a large loading capacity. MSNs can be modified into bulk materials with well-controlled nano- or micrometric particle sizes, with MCM-41 being the most commonly used for the treatment of bacterial infections. MSNs have the advantage of producing materials of various sizes and pore diameters by altering the synthesis conditions,

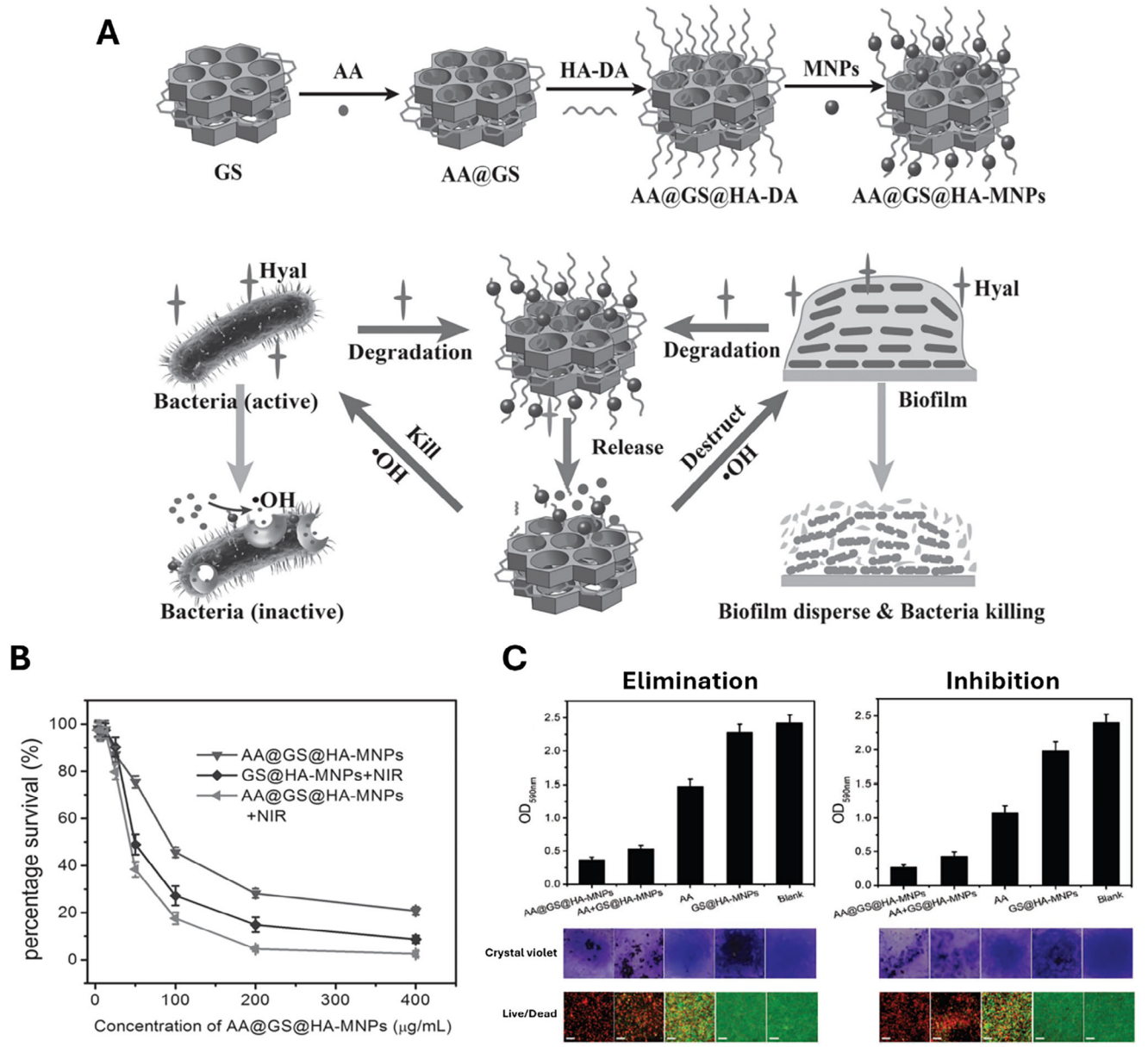

Figure 9. Bacterial hyaluronidase-responsive prodrug release for chemo-photothermal synergistic antibacterial therapy. A) Schematic representation of the synthesis of AA@GS@HA-MNPs and their mechanism of action. Drug release is triggered by bacterial hyaluronidase, enabling site-specific activation. B) Survival rates of *S. aureus* following treatment with AA@GS@HA-MNPs, GS@HA-MNPs with photothermal irradiation, and AA@GS@HA-MNPs with photothermal irradiation (808 nm, 6 W/cm^2, 5 min). C) Evaluation of the antibacterial system based on GS@HA-MNPs for the elimination and inhibition of *S. aureus* biofilm formation. Quantification of remaining biofilm was performed using crystal violet staining (mean ± SD, $n = 3$). Representative images of biofilms stained with crystal violet and fluorescence microscopy images of residual biofilms stained with LIVE/DEAD viability stain. Green and red fluorescence indicate live and dead bacteria, respectively. Scale bar = 10 μm. Reproduced with permission.[180] Copyright 2016, Wiley.

allowing them to load not only small molecules but also large proteins.[184,185] Another important property of MSNs is their potential for easy surface functionalization to achieve targeted and triggered drug release. Two distinct triggering mechanisms can be identified: internal factors (pH, redox, enzymes, etc.) and external factors (photochemical, thermal, magnetic, etc.).[186] Different functional groups can be grafted onto the silica surface to carry drugs with distinct charges.[187]

Passive release of antimicrobials from MSNs can unintentionally occur in the circulatory system while traveling to the infection site, causing undesirable secondary effects along the way. However, selective delivery of antimicrobials to the target location with a controlled release profile can be achieved through two main strategies. The first involves functionalizing the MSNs with passive or active targeting mechanisms, typically by grafting selective ligands onto their external surfaces. For example, antibodies

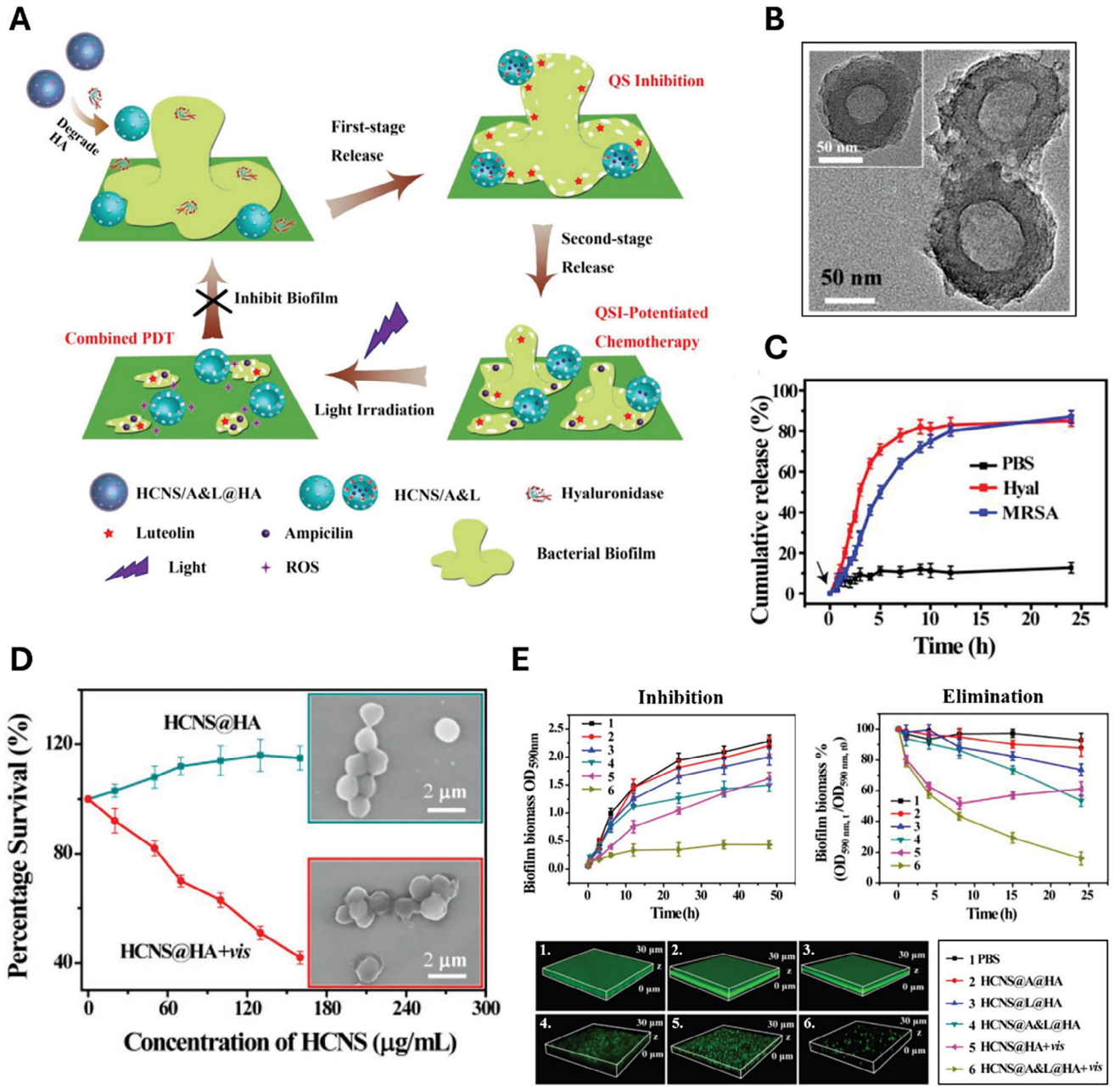

Figure 10. Integration of QS inhibition and photodynamic therapy using a multidrug-loaded hollow carbon nitride sphere system. A) Schematic illustration of the bacterial enzyme-responsive nanosystem (HCNS@HA), designed to disperse biofilms by QS inhibition, enhance antibiotic efficacy, and enable synergistic photodynamic treatment. B) TEM image of HCNS@HA nanoparticles showing their hollow spherical morphology. C) Cumulative release profile of luteolin from HCNS/L@HA in PBS buffer under three conditions: without hyaluronidase (black line), with hyaluronidase (150 U/mL, red line), and in the presence of MRSA (blue line). D) Viability of MRSA treated with various concentrations of HCNS@HA under photodynamic therapy. Insets: SEM images of MRSA post-treatment. E) Anti-biofilm effects of HCNS@HA-based treatments, including biofilm elimination and inhibition. Treatment used [HCNS] = 600 μg mL^{-1}. Confocal laser scanning microscopy images show biofilm formation on untreated and pretreated surfaces after 24 h incubation. Biofilms were stained with fluorescein (Image size: 315.76 μm × 315.76 μm). Reproduced with permission.[23] Copyright 2019, Wiley.

or vancomycin can be used to target teichoic acid and peptidoglycan in Gram-positive bacteria,[188] while polymyxin can selectively target lipopolysaccharides in Gram-negative bacteria.[189]

Using this approach, Velikova et al. loaded mesoporous MCM-41 NPs with vancomycin, and functionalized these particles with two-component system histidine kinase autophosphorylation inhibitors (HKAIs), and then they coated them with e-poly-L-lysine (ePLL).[190] The coating promoted ionic bonding with the negatively charged bacterial outer membrane and facilitated the membrane permeation of vancomycin. The system exhibited strong bactericidal activity against both Gram-positive and Gram-negative bacteria due to the enhanced delivery and

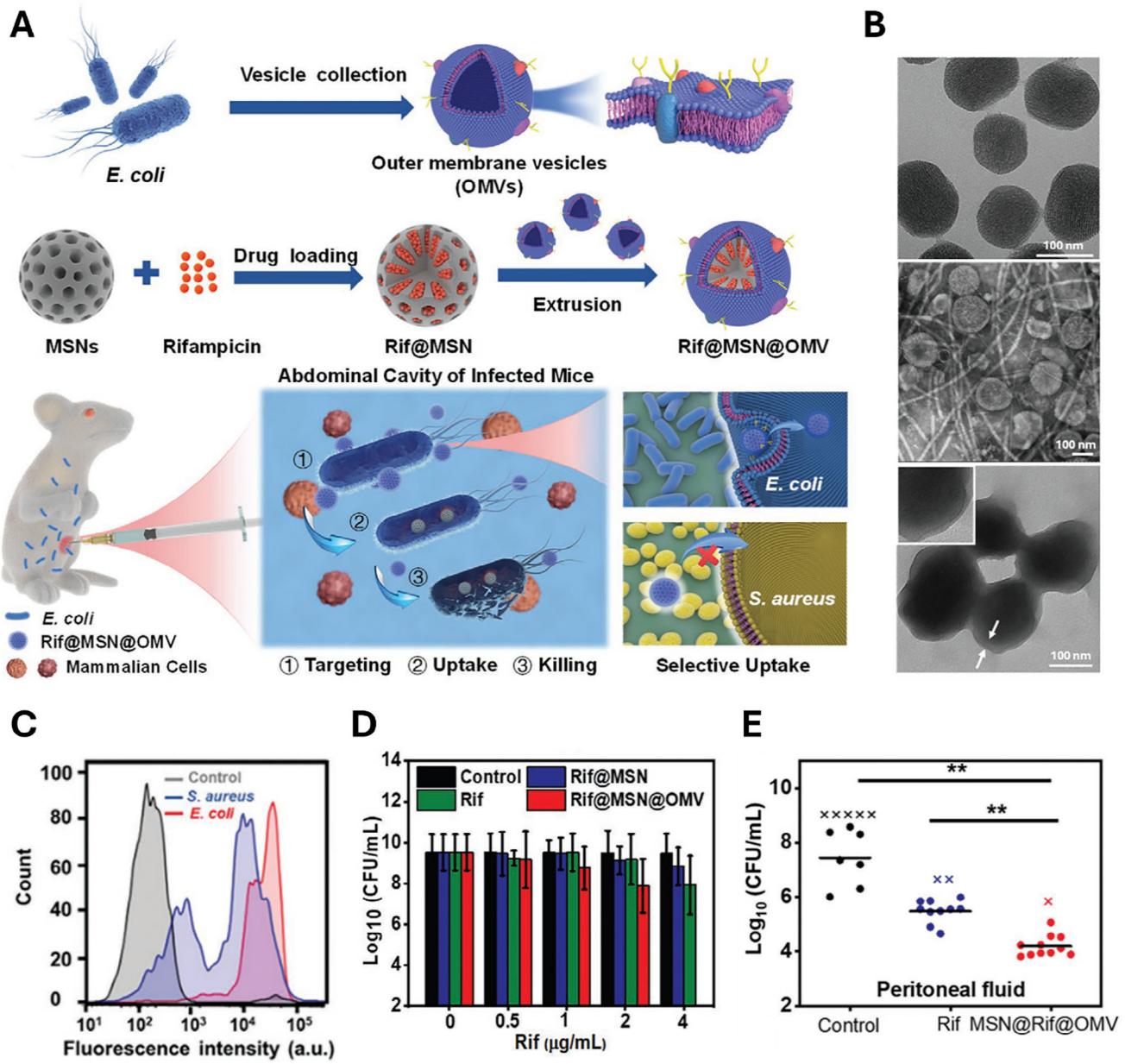

Figure 11. Bacterial outer membrane-coated mesoporous silica nanoparticles for targeted rifampicin delivery against Gram-negative bacterial infection in vivo. A) Schematic illustration of the synthesis and therapeutic mechanism of the biomimetic nanosystem Rif@MSN@OMV. Mesoporous silica nanoparticles loaded with rifampicin were coated with *E. coli* OMVs to form Rif@MSN@OMV. In a mouse model of *E. coli*-induced peritonitis, Rif@MSN@OMV demonstrated enhanced antimicrobial efficacy compared to free rifampicin, owing to improved bacterial targeting and selective uptake by *E. coli*, with minimal interaction with non-target cells, including *S. aureus*. B) TEM images of MSNs (top), OMVs (middle), and the hybrid MSN@OMV particles (bottom). C) Flow cytometry analysis of cellular uptake of MSN@OMV in *E. coli* and *S. aureus*, showing selective internalization. D) Quantification of bacterial CFUs after 24 h incubation with Rif@MSN@OMV, Rif@MSN, and free rifampicin at various concentrations ($n = 3$). E) In vivo antibacterial efficacy of Rif@MSN@OMV in a mouse model of *E. coli*-induced peritonitis. Bacterial CFUs in peritoneal fluid of untreated mice, mice treated with free rifampicin, and mice treated with Rif@MSN@OMV ($n = 12$). "×" symbols indicate mice that died within 24 h post-infection. $p < 0.05$, $p < 0.01$. Reproduced with permission.[191] Copyright 2021, Wiley.

internalization of the HKAIs. The toxicity of the prepared materials was tested in vivo using zebrafish larvae, which showed no adverse effects on the embryos at the doses tested.

In the same line, Wu et al. developed a targeted antibiotic delivery system by coating MSNs loaded with rifampicin using outer membrane vesicles (OMVs) derived from *E. coli*, forming Rif@MSN@OMVs, as shown in **Figure 11**.[191] The successful functionalization was confirmed by an increase in their particle size and an adequate surface zeta potential. Cellular uptake studies using confocal microscopy and flow cytometry showed that the OMV-coated MSNs exhibited significantly greater cellular internalization in *E. coli* compared to *S. aureus*,

consistent with the OMV source. Antibacterial assays conducted in vitro demonstrated that while free rifampicin, Rif@MSN, and Rif@MSN@OMV were administered at identical concentrations (4 μg mL^{-1}), only the OMV-coated formulation achieved a near-complete bactericidal effect. In vivo experiments using a murine peritonitis model further validated these findings. A single intraperitoneal dose of Rif@MSN@OMV (0.2 mg mL^{-1} Rif equivalent) led to a 3 reduction in *E. coli* load in peritoneal fluid, significantly outperforming free rifampicin. Additionally, the OMV-targeted formulation was more effective at reducing bacterial burden in major organs, including the spleen, kidneys, and lungs, and contributed to a higher survival rate in infected mice. These results highlight the potential of bacterial vesicle-coated MSNs for systemically targeted, infection-responsive antibiotic delivery.

Other strategies including MSNs involve capping the pores with materials or mechanisms designed to retain the entrapped cargo within the MSN, releasing it only in response to specific external stimuli.[192] These gated MSNs have been used for the controlled release of drugs in bactericidal applications. The design of gated mesoporous supports that deliver their cargo under specific environmental conditions has proven to be an effective approach for developing smart antimicrobial applications.[193] For instance, MSNs were employed to develop a pH-responsive ampicillin carrier with folic acid and calcium phosphate (CaP) coating.[194] The folic acid was first modified and then covered with CaP through a chelating effect and biomineralization. The CaP controlled the antibiotic release in response to pH changes. An additional layer of FA was added to create a nanocomposite that enhances antibacterial activity by overcoming the efflux pump system of drug-resistant bacteria. The targeting ability of the FA-coated composite to anti-inflammatory zones was tested in mice infected with bacteria, showing a fast promotion of wound healing.

Lastly, MSNs can be combined with other materials to gain enhanced properties for multifunctional applications. For example, integrating MSNs with materials like Au or Ag NPs, QDs, or specific polymers can create a synergistic antimicrobial effect, amplifying their efficacy when used alongside standard antimicrobials.[195,196]

3.4.3. Clay Derived Nanomaterials

Natural occurring clay minerals have been used in the field of health products since ancient times.[197] Today, clays are incorporated into oral medications as antacids, gastrointestinal protectants, and antidiarrheals due to their low toxicity when administered orally. The structural unit of montmorillonite clay—the primary constituent of bentonite—is composed of two silicon oxytetrahedral layers and an aluminum octahedral layer sandwiched between them. These layers are held together by van der Waals forces and electrostatic interactions. Montmorillonite can readily adsorb drugs due to its large specific surface area, high adsorption capacity, swelling properties, and substantial cation exchange capacity. The strong interactions between the clay and the drugs result in slow, sustained release, making these materials effective for targeted drug delivery.

The interaction between EPS secreted by bacteria and inorganic minerals involves a variety of intermolecular forces, including hydrophobic, electrostatic, and covalent interactions.[198] This natural adsorption phenomenon was used to design an antimicrobial clay with bacteria-cell-specific adhesive properties. This natural adsorption phenomenon was leveraged to design an antimicrobial clay with bacteria-specific adhesive properties. Montmorillonite has been shown to attach to bacterial extracellular polymers and also exhibits mucoadhesive properties that facilitate passage across gastrointestinal barriers. Highly exfoliated montmorillonite was modified with cationic linear polyethyleneimine to enhance bacterial adhesion and disrupt cell membranes.[198] These exfoliated montmorillonite nanosheets possess a high surface area that promotes bacterial adhesion, while the cationic polymer contributes to membrane disruption. Metronidazole was incorporated into the exfoliated clay via ion-exchange prior to polymer functionalization. The resulting material effectively eliminated *Helicobacter pylori* SS1 in infected athymic female mice with peptic ulcers.

3.4.4. Calcium-Derived Nanomaterials

Porous calcium carbonate is suitable as a drug carrier, especially in bone scaffolds, because of its osteoconductive properties and bone-forming activity.[199] Calcium carbonate is present in different forms, including calcite, aragonite, and vaterite; this last polymorph is used the most because it has large porosity and a large surface area. These properties provide vaterite with high loading capacity, improved PK profile, and, besides, it has the possibility to load lipophilic drugs. Calcium carbonate's porous structure is also sensitive to the environmental pH, making vaterite particles attractive for their use as pH-responsive drug delivery systems.[186]

In the study by Min et al., doxycycline-loaded calcium carbonate NPs were fabricated by a mineralization process to deliver the antibiotic to bacterial virulent biofilms.[200] Calcium carbonate NPs were loaded with doxycycline during mineral nucleation and growth. The antibiotic was held in the carbonate core at physiological pH and released within the acidic microenvironment of bacteria biofilms. The material presented inhibitory effects on *Prevotella intermedia* ATCC49046 biofilms proliferation and formation.

3.4.5. Other Inorganic Materials

Polyoxometalates (POMs) are inorganic clusters of metal ions connected through oxygen atoms, having catalytic and redox ability which have also been used as antimicrobial triggerable materials. For example, Zhao et al. developed a nanoparticulated dually-responsive antibiofilm system triggered by the acidic conditions of the infection site and having, in addition, the ability to activate its photothermal properties in response to the presence of bacterial H_2S.[201] This molybdenum-based POM nanocluster doped with copper was validated in an implant-related periprosthetic *S. aureus* infection murine model for selective antibiofilm therapy. Under the acidic biofilm conditions, the nanocluster produced antibacterial molecules through bioorthogonal reactions, and under simulated high concentrations of NaHS the clusters increased their NIR absorption in the second near-infrared region, facilitating their photothermal antibiofilm effect.

Table 5. Non-metal inorganic nanomaterials for the management of bacterial infections.

Material	Composition	Other components	Antimicrobial	Size [nm]	Bacteria	Effect	Refs.
CBM	Graphene, mesoporous silica	Hyaluronic acid, dopamine	Ascorbic acid	100 – 300	*S. aureus*	Responsive chemo-photothermal antibacterial and antibiofilm therapy	[180]
CBM	Carbon nitride	Hyaluronic acid	Ampicillin, Luteonin	≈132	MRSA	Responsive and photothermal therapy. Biofilm eradication	[23]
MSN	MCM-41	ϵ-poly-L-lysine	HKAIs	≈100	*E. coli* *S. marcescens*	HKAIs enhanced activity	[190]
MSN	MCM-41	pNIPAAm-co-pAEMA copolymer, peptide ligands	Tobramycin	≈1000	*P. mirabillis* *B. subtilis*	Bacterial motility triggered release	
MSN	Mesoporous silica	Folic acid, CaP	Ampicillin	≈120	*E. coli* *S. aureus*	pH responsive, theragnostic applications	[194]
MSN	Mesoporous silica	PEI, Cyclodextrin-based-pH-valves	Isoniazid, Rifampin	≈100	*M. tuberculosis*	Intracellular infection treatment	[202]
MSN	Mesoporous silica	Arg	Ciprofloxacin	≈75	*S. typhimurium*	Intracellular infection treatment	[203]
MSN	Mesoporous silica	–	Lysostaphin, serrapeptase, DNase I	≈36	*S. aureus* MRSA	Biofilm disruption	[204]
MSN	Mesoporous silica	Gold nanorods	Levofloxacin, NO	≈100	*S. aureus*	Biofilm disruption	[205]
Mesoporous silica	Mesoporous silica	FITC	Vancomycin	90 ± 37	*S. aureus*	Intracellular infection treatment, Theragnostic applications	[188]
Clay	Montmorillonite	PEI	Metronidazole	400 – 900	*H. pylori*	Targeted antimicrobial delivery	[198]
Calcium	$CaCO_3$	–	Doxycycline	≈312	*P. intermedia*	pH responsive sustained release	[200]
POM	molybdenum (Mo)-based POM nanoclusters	Doped with Cu	Cu-click reaction on prodrugs to produce bisamidine analoges	≈70	*S. aureus*	Biofilm elimination	[201]

Table 5 presents a selection of studies, including those described in the text and others, that use non-metal inorganic nanomaterials for the treatment of bacterial infections.

4. Conclusion

A thorough understanding of unique signaling elements present or released by bacteria combined with the rational design of targeted nanobased drug delivery systems, is key to developing nanostructured systems that outperform conventional passive or non-targeted approaches. The release of the antimicrobial drug in response to the presence of specific pathogenic bacteria supports a rational usage of antimicrobials, avoiding incorrect dosing, favors patient´s compliance, and matches with the bacterial growth dynamics and status, ultimately improving treatment results and reducing the chances of developing resistance. Bacteria well-conserved and ubiquitous cell-specific moieties such as membrane proteins, quenchers of signaling molecules (e.g., AHL inhibitors, luteolin), adhesins, antimicrobial peptides, iron-mimics, proteases, DNAses, glycoside hydrolases, glycolipids present in the bacterial biofilm architecture, bacterial toxins, acidic cues, bacterial enzymes (e.g., lipase, lactate dehydrogenase, hyaluronidase, etc.), exopolysaccharides (e.g., EPSs) and so on, have been used as targeting ligands toward which nanostructured carriers loaded or surface grafted with antimicrobial compounds are designed for infection-specific on-demand antimicrobial therapy. These systems enhance the availability of hydrophobic antimicrobials, offer superior protection against physiological degradation, and extend the duration of antimicrobial action—thereby reducing dosing frequency and preventing rapid clearance from the body. Some of these nanomaterials possess intrinsic antimicrobial properties, while others combine multiple drugs within a single carrier, boosting the bactericidal effect and minimizing the concentration required to inhibit or eradicate pathogenic bacteria. These responsive nanosystems can eliminate planktonic, sessile, and intracellular bacteria in their various phenotypic states, and can even interfere with signaling and communication molecules released by bacteria. Overall, the development of targeted and responsive nanosystems that release multiple antimicrobial agents in response to bacterial presence—while minimizing side effects—represents an efficient strategy to combat antimicrobial resistance. Further efforts are required

to demonstrate that those proposed infection-specific on-demand antimicrobial release carriers reduce resistance compared to conventional passive or continuous delivery systems. Also a cost analysis should guarantee that the proposed nano-based technologies can be universally adopted at a reasonable cost. The rapid advances in artificial intelligence-driven diagnostics combined with genomics will help in the design of custom antimicrobial nanobased carriers with enhanced effectiveness. Nanoparticulated systems that monitor in real time treatment outcome represent one of the novel advances to aid in the rapid change of one antimicrobial regime when ineffective, ultimately avoiding resistance.

Acknowledgements

The authors acknowledge the Spanish Ministry of Science, Innovation and Universities (grant number PID2023-146091OB-I00) for funding, and for the Severo Ochoa Programme for Centers of Excellence in R&D (CEX2023-001286-S MICIU/AEI/10.13039/501100011033). The authors also thank the Aragon Government for the grant PROY_B21_24. The authors acknowledge the financial support from Instituto de Salud Carlos III (Spain; Fortalece Call, grant number FORT23/00028). G.M. gratefully acknowledges the support from the Miguel Servet Program (MS19/00092; Instituto de Salud Carlos III). Some of the figures in this manuscript were created using BioRender.com with appropriate licensing.

Conflict of Interest

The authors declare no conflict of interest.

Declaration of Generative AI and AI-Assisted Technologies in the Writing Process

During the preparation of this work, the authors used ChatGPT in order to check and refine the grammar and clarity of the text. After using this tool, the authors reviewed and edited the content as needed and take full responsibility for the content of the published article.

Keywords

bacterial infections, biofilm, drug delivery systems, nanostructured materials, quorum sensing, targeted antimicrobial treatments

Received: June 6, 2025
Revised: July 29, 2025
Published online:

[1] A. Yarahmadi, H. Najafiyan, M. H. Yousefi, E. Khosravi, E. Shabani, H. Afkhami, S. S. Aghaei, *Front. Cell Infect Microbiol.* **2025**, *15*, 1493915.
[2] M. Naghavi, S. E. Vollset, K. S. Ikuta, L. R. Swetschinski, A. P. Gray, E. E. Wool, G. Robles Aguilar, T. Mestrovic, G. Smith, C. Han, R. L. Hsu, J. Chalek, D. T. Araki, E. Chung, C. Raggi, A. Gershberg Hayoon, N. Davis Weaver, P. A. Lindstedt, A. E. Smith, U. Altay, N. V. Bhattacharjee, K. Giannakis, F. Fell, B. McManigal, N. Ekapirat, J. A. Mendes, T. Runghien, O. Srimokla, A. Abdelkader, S. Abd-Elsalam, et al., *Lancet* **2024**, *404*, 1199.
[3] Centers for Disease Control and Prevention (CDC). More People in the United States Dying from Antibiotic-Resistant Infections than Previously Estimated, CDC Online Newsroom, **2019**. https://archive.cdc.gov/#/details?url=https://www.cdc.gov/media/releases/2019/p1113-antibiotic-resistant.html (accessed: December 2021).
[4] E. Y. Klein, T. P. Van Boeckel, E. M. Martinez, S. Pant, S. Gandra, S. A. Levin, H. Goossens, R. Laxminarayan, *Proc. Natl. Acad. Sci. USA* **2018**, *115*, 3463.
[5] E. K. Sully, B. L. Geller, L. Li, C. M. Moody, S. M. Bailey, A. L. Moore, M. Wong, P. Nordmann, S. M. Daly, C. R. Sturge, D. E. Greenberg, *J. Antimicrob. Chemother.* **2017**, *72*, 782.
[6] S. J. Lam, N. M. O'Brien-Simpson, N. Pantarat, A. Sulistio, E. H. H. Wong, Y.u-Y. Chen, J. C. Lenzo, J. A. Holden, A. Blencowe, E. C. Reynolds, G. G. Qiao, *Nat. Microbiol.* **2016**, *1*, 16162.
[7] C. K. Lee, J. de Anda, A. E. Baker, R. R. Bennett, Y. Luo, E. Y. Lee, J. A. Keefe, J. S. Helali, J. Ma, K. Zhao, R. Golestanian, G. A. O'Toole, G. C. L. Wong, *Proc. Natl. Acad. Sci. USA* **2018**, *115*, 4471.
[8] C. De la Fuente-Núñez, F. Reffuveille, L. Fernández, R. E. W. Hancock, *Curr. Opin. Microbiol.* **2013**, *16*, 580.
[9] B. M. Peters, M. A. Jabra-Rizk, G. A. O'May, J. William Costerton, M. E. Shirtliff, *Clin. Microbiol. Rev.* **2012**, *25*, 193.
[10] B. Singha, V. Singh, V. Soni, *Front. Drug Discov.* **2024**, *4*, 1385460.
[11] V. Johnson, T. Webb, A. Norman, J. Coy, J. Kurihara, D. Regan, S. Dow, *Sci. Rep.* **2017**, *7*, 9575.
[12] A. Estellés, A.-K. Woischnig, K. Liu, R. Stephenson, E. Lomongsod, D.a Nguyen, J. Zhang, M. Heidecker, Y. Yang, R. J. Simon, E. Tenorio, S. Ellsworth, A. Leighton, S. Ryser, N. K. Gremmelmaier, L. M. Kauvar, *Antimicrob. Agents Chemother.* **2016**, *60*, 2292.
[13] S. M. Barksdale, E. J. Hrifko, M. L. van Hoek, *Dev. Comp. Immunol.* **2017**, *70*, 135.
[14] H. Leonard, R. Colodner, S. Halachmi, E. Segal, *ACS Sens.* **2018**, *3*, 2202.
[15] Z. A. Khan, M. F. Siddiqui, S. Park, *Diagnostics* **2019**, *9*, 49.
[16] N. Høiby, T. Bjarnsholt, C. Moser, G. L. Bassi, T. Coenye, G. Donelli, L. Hall-Stoodley, V. Holá, C. Imbert, K. Kirketerp-Møller, D. Lebeaux, A. Oliver, A. J. Ullmann, C. Williams, *Clin Microbiol. Infect.* **2015**, *21*.
[17] P. V. Baptista, M. P. McCusker, A. Carvalho, D. A. Ferreira, N. M. Mohan, M. Martins, A. R. Fernandes, *Front. Microbiol.* **2018**, *9*, 1441.
[18] K. Kalishwaralal, S. BarathManiKanth, S. R. K. Pandian, V. Deepak, S. Gurunathan, *Colloids Surf B Biointerfaces* **2010**, *79*, 340.
[19] A. M. Allahverdiyev, K. V. Kon, E. S. Abamor, M. Bagirova, M. Rafailovich, *Expert Rev. Anti Infect Ther.* **2011**, *9*, 1035.
[20] A. León-Buitimea, C. R. Garza-Cárdenas, J. A. Garza-Cervantes, J. A. Lerma-Escalera, J. R. Morones-Ramírez, *Front. Microbiol.* **2020**, *11*, 1669.
[21] D. Hu, H. Li, B. Wang, Z. Ye, W. Lei, F. Jia, Q. Jin, K. F. Ren, J. Ji, *ACS Nano* **2017**, *11*, 9330.
[22] W. Bing, Z. Chen, H. Sun, P. Shi, N. Gao, J. Ren, X. Qu, *Nano Res.* **2015**, *8*, 1648.
[23] Y. Sun, H. Qin, Z. Yan, C. Zhao, J. Ren, X. Qu, *Adv. Funct. Mater.* **2019**, *29*, 1808222.
[24] Y. Xi, J. Ge, M. Wang, M. Chen, W. Niu, W. Cheng, Y. Xue, C. Lin, B. Lei, *ACS Nano* **2020**, *14*, 2904.
[25] J. Zhou, A. L. Loftus, G. Mulley, A. T. A. Jenkins, *J. Am. Chem. Soc.* **2010**, *132*, 6566.
[26] N. T. Thet, D. R. Alves, J. E. Bean, S. Booth, J. Nzakizwanayo, A. E. R. Young, B. V. Jones, A. T. A. Jenkins, *ACS Appl. Mater. Interfaces* **2016**, *8*, 14909.
[27] S. Rao C V, E. De Waelheyns, A. Economou, J. Anné, *Biochim Biophys Acta Mol Cell Res* **2014**, *1843*, 1762.
[28] Y. Hsieh, H. Zhang, B. Lin, N. Cui, B. Na, H. Yang, C. Jiang, S. Sui, P. C. Tai, *J. Biol. Chem.* **2011**, *286*, 44702.

[29] M. Y. Jang, S. D.e Jonghe, K. Segers, J. Anné, P. Herdewijn, *Bioorg. Med. Chem.* **2011**, *19*, 702.
[30] E. De Waelheyns, K. Segers, M. F. Sardis, J. Anné, G. A. F. Nicolaes, A. Economou, *J. Antibiot.* **2015**, *68*, 666.
[31] R. E. Dalbey, M. O. Lively, S. Bron, J. M. Van Dijl, *Protein Sci.* **1997**, *6*, 1129.
[32] A. Gupta, S. Mumtaz, C. H. Li, I. Hussain, V. M. Rotello, *Chem. Soc. Rev.* **2019**, *48*, 415.
[33] Y. Sakuragi, R. Kolter, *J. Bacteriol.* **2007**, *189*, 5383.
[34] M. Allesen-Holm, K. B. Barken, L. Yang, M. Klausen, J. S. Webb, S. Kjelleberg, S. Molin, M. Givskov, T. Tolker-Nielsen, *Mol. Microbiol.* **2006**, *59*, 1114.
[35] F. Rezzonico, B. Duffy, *BMC Microbiol.* **2008**, *8*, 154.
[36] R. P. Novick, E. Geisinger, *Annu. Rev. Genet.* **2008**, *42*, 541.
[37] B. R. Boles, A. R. Horswill, *PLoS Pathog.* **2008**, *4*, 1000052.
[38] K. Sambanthamoorthy, R. E. Sloup, V. Parashar, J. M. Smith, E. E. Kim, M. F. Semmelhack, M. B. Neiditch, C. M. Waters, *Antimicrob. Agents Chemother.* **2012**, *56*, 5202.
[39] Y. Jiang, M. Geng, L. Bai, *Microorganisms* **2020**, *8*, 1222.
[40] C. N. Spaulding, R. D. Klein, S. Ruer, A. L. Kau, H. L. Schreiber, Z. T. Cusumano, K. W. Dodson, J. S. Pinkner, D. H. Fremont, J. W. Janetka, H. Remaut, J. I. Gordon, S. J. Hultgren, *Nature* **2017**, *546*, 528.
[41] Z. Han, J. S. Pinkner, B. Ford, R. Obermann, W. Nolan, S. A. Wildman, D. Hobbs, T. Ellenberger, C. K. Cusumano, S. J. Hultgren, J. W. Janetka, *J. Med. Chem.* **2010**, *53*, 4779.
[42] Y. Kaneko, M. Thoendel, O. Olakanmi, B. E. Britigan, P. K. Singh, *J. Clin. Invest.* **2007**, *117*, 877.
[43] P. Stoodley, K. Sauer, D. G. Davies, J. W. Costerton, *Annu. Rev. Microbiol.* **2002**, *56*, 187.
[44] T. F. C. Mah, G. A. O'Toole, *Trends Microbiol.* **2001**, *9*, 34.
[45] J. S. Gunn, L. O. Bakaletz, D. J. Wozniak, *J. Biol. Chem.* **2016**, *291*, 12538.
[46] J. Bouckaert, J. Berglund, M. Schembri, E. De Genst, L. Cools, M. Wuhrer, C.-S. Hung, J. Pinkner, R. Slättegård, A. Zavialov, D. Choudhury, S. Langermann, S. J. Hultgren, L. Wyns, P. Klemm, S. Oscarson, S. D. Knight, H. De Greve, *Mol. Microbiol.* **2005**, *55*, 441.
[47] L. Hall-Stoodley, L. Nistico, K. Sambanthamoorthy, B. Dice, D. Nguyen, W. J. Mershon, C. Johnson, F. Ze Hu, P. Stoodley, G. D. Ehrlich, J. C. Post, *BMC Microbiol.* **2008**, *8*, 173.
[48] K. Nemoto, K. Hirota, K. Murakami, K. Taniguti, H. Murata, D. Viducic, Y. Miyake, *Chemotherapy* **2003**, *49*, 121.
[49] M. Schmelcher, Y. Shen, D. C. Nelson, M. R. Eugster, F. Eichenseher, D. C. Hanke, M. J. Loessner, S. Dong, D. G. Pritchard, J. C. Lee, S. C. Becker, J. Foster-Frey, D. M. Donovan, *J. Antimicrob. Chemother.* **2015**, *70*, 1453.
[50] D. Fleming, L. Chahin, K. Rumbaugh, *Antimicrob. Agents Chemother.* **2017**, *61*,.
[51] S. Choi, M. A. Hassan, B. E. Britigan, P. Narayanasamy, *Curr. Issues Mol. Biol.* **2024**, *46*, 9149.
[52] K. Papenfort, B. L. Bassler, *Nat. Rev. Microbiol.* **2016**, *14*, 576.
[53] R. S. Kalhapure, N. Suleman, C. Mocktar, N. Seedat, T. Govender, *J. Pharm. Sci.* **2015**, *104*, 872.
[54] D.-Y. Wang, H. C. van der Mei, Y. Ren, H. J. Busscher, L. Shi, *Front. Chem.* **2020**, *7*, 872.
[55] Y. Liu, L. Shi, L. Su, H. C. van der Mei, P. C. Jutte, Y. Ren, H. J. Busscher, *Chem. Soc. Rev.* **2019**, *48*, 428.
[56] T. M. Allen, P. R. Cullis, *Adv. Drug. Deliv. Rev.* **2013**, *65*, 36.
[57] L. Sercombe, T. Veerati, F. Moheimani, S. Y. Wu, A. K. Sood, S. Hua, *Front. Pharmacol.* **2015**, *6*, 286.
[58] D. Cipolla, J. Blanchard, I. Gonda, *Pharmaceutics* **2016**, *8*, 6.
[59] A. Pumerantz, K. Muppidi, S. Agnihotri, C. Guerra, V. Venketaraman, J. Wang, G. Betageri, *Int. J. Antimicrob. Agents* **2011**, *37*, 140.
[60] S. Wang, S. Yu, Y. Lin, P. Zou, G. Chai, H. H. Yu, H. Wickremasinghe, N. Shetty, J. Ling, J. Li, Q.i Zhou, *Pharm. Res.* **2018**, *35*, 187.
[61] P. Deol, G. K. Khuller, K. Joshi, *Antimicrob. Agents Chemother.* **1997**, *41*, 1211.
[62] R. S. Santos, C. Figueiredo, N. F. Azevedo, K. Braeckmans, S. C. De Smedt, *Adv Drug Deliv Rev* **2018**, *136–137*, 28.
[63] R. S. Santos, G. R. Dakwar, E. Zagato, T. Brans, C. Figueiredo, K. Raemdonck, N. F. Azevedo, S. C. De Smedt, K. Braeckmans, *Biomaterials* **2017**, *138*, 1.
[64] D. Nicolosi, M. Scalia, V. M. Nicolosi, R. Pignatello, *Int. J. Antimicrob. Agents* **2010**, *35*, 553.
[65] W. S. Cheow, K. Hadinoto, *Particuology* **2012**, *10*, 327.
[66] Y. Wu, Z. Song, H. Wang, H. Han, *Nat. Commun.* **2019**, *10*, 4464.
[67] C. A. Omolo, N. A. Megrab, R. S. Kalhapure, N. Agrawal, M. Jadhav, C. Mocktar, S. Rambharose, K. Maduray, B. Nkambule, T. Govender, *J. Liposome Res.* **2021**, *22*, 347.
[68] M. M. Fabani, R. Gargini, M. C. Taira, R. Iacono, S. Alonso-Romanowski, *J. Liposome Res.* **2002**, *12*, 13.
[69] X. Hou, X. Zhang, W. Zhao, C. Zeng, B. Deng, D. W. McComb, S. Du, C. Zhang, W. Li, Y. Dong, *Nat. Nanotechnol.* **2020**, *15*, 41.
[70] V. Mishra, K. K. Bansal, A. Verma, N. Yadav, S. Thakur, K. Sudhakar, J. M. Rosenholm, *Pharmaceutics* **2018**, *10*, 191.
[71] N. E. Eleraky, A. Allam, S. B. Hassan, M. M. Omar, *Pharmaceutics* **2020**, *12*.
[72] R. H. Müller, K. Mäder, S. Gohla, *Eur. J. Pharm. Biopharm.* **2000**, *50*, 161.
[73] C. R. Thorn, N. Thomas, B. J. Boyd, C. A. Prestidge, *Drug Deliv. Transl. Res.* **2021**, *11*, 1598.
[74] R. S. Kalhapure, D. R. Sikwal, S. Rambharose, C. Mocktar, S. Singh, L. Bester, J. K. Oh, J. Renukuntla, T. Govender, *Nanomedicine* **2017**, *13*, 2067.
[75] C. R. Thorn, C. Carvalho-Wodarz, S. de, J. C. Horstmann, C. M. Lehr, C. A. Prestidge, N. Thomas, *Small* **2021**, *17*, 2100531.
[76] H.-W. An, Y. Fei, T.-D.a Yan, C.-Q.i Lu, M.-D.i Wang, T. Ma, B.o-Y. Zhao, J.-M. Nie, H.-R. Tseng, L.i-L.i Li, H. Wang, *Adv. Ther.* **2020**, *3*, 1900217.
[77] R. E. Alarfaj, M. M. Alkhulaifi, A. J. Al-Fahad, S. Aljihani, A. E. B. Yassin, M. F. Alghoribi, M. A. Halwani, *Pharmaceutics* **2022**, *14*, 130.
[78] M. Jadhav, R. S. Kalhapure, S. Rambharose, C. Mocktar, S. Singh, T. Kodama, T. Govender, *Chem. Phys. Lipids* **2018**, *212*, 12.
[79] Q. Zhou, J. Wang, Y. Liang, H. Yang, Q. Li, Q. Li, D. Liao, Y. Liu, H. B. Liu, *Chem. Nano. Mat.* **2020**, *6*, 516.
[80] S. Yu, S. Wang, P. Zou, G. Chai, Y.-W. Lin, T. Velkov, J. Li, W. Pan, Q. T. Zhou, *Int. J. Pharm.* **2020**, *575*, 118915.
[81] Y.u Wang, Q. Yuan, W. Feng, W. Pu, J. Ding, H. Zhang, X. Li, B.o Yang, Q. Dai, L. Cheng, J. Wang, F. Sun, D. Zhang, *J. Nanobiotechnol.* **2019**, *17*, 1.
[82] H. Akhtari, B. S. Fazly Bazzaz, S. Golmohammadzadeh, J. Movaffagh, V. Soheili, B. Khameneh, *J. Pharm. Innov.* **2021**, *16*, 293.
[83] J. Liu, J. Meng, L. Cao, Y. Li, P. Deng, P. Pan, C. Hu, H. Yang, *J. Photochem. Photobiol. B* **2019**, *197*, 111510.
[84] N. Nafee, A. Husari, C. K. Maurer, C. Lu, C. De Rossi, A. Steinbach, R. W. Hartmann, C. M. Lehr, M. Schneider, *J. Control Release* **2014**, *192*, 131.
[85] E. N. Taylor, K. M. Kummer, D. Dyondi, T. J. Webster, R. Banerjee, *Nanoscale* **2014**, *6*, 825.
[86] S. M. Hosseini, A. Farmany, R. Abbasalipourkabir, S. Soleimani Asl, A. Nourian, M. R. Arabestani, *Ann. Clin. Microbiol. Antimicrob.* **2019**, *18*, 1.
[87] S. Alarifi, S. Massadeh, M. Al-Agamy, M. Al Aamery, A. Al Bekairy, A. E. Yassin, *Trop. J. Pharm. Res.* **2020**, *19*, 909.
[88] D. P. C. de Barros, R. Santos, P. Reed, L. P. Fonseca, A. Oliva, *Molecules* **2022**, *27*, 8818.
[89] S. E. Alavi, U. Bakht, M. Koohi Moftakhari Esfahani, H. Adelnia, S. H. Abdollahi, H. Ebrahimi Shahmabadi, A. Raza, *Pharmaceutics* **2022**, *14*, 1668.

[90] M. A. Beach, U. Nayanathara, Y. Gao, C. Zhang, Y. Xiong, Y. Wang, G. K. Such, *Chem. Rev.* **2024**, *124*, 5505.
[91] P. Lai, W. Daear, R. Löbenberg, E. J. Prenner, *Colloids Surf B Biointerfaces* **2014**, *118*, 154.
[92] A. Cano, M. Ettcheto, M. Espina, A. López-Machado, Y. Cajal, F. Rabanal, E. Sánchez-López, A. Camins, M. L. García, E. B. Souto, *J. Nanobiotechnol.* **2020**, *18*, 1.
[93] A. K. Shakya, M. Al-Sulaibi, R. R. Naik, H. Nsairat, S. Suboh, A. Abulaila, *Polymers* **2023**, *15*, 3597.
[94] Y. Yang, Y. Ding, B. Fan, Y. Wang, Z. Mao, W. Wang, J. Wu, *J. Control Release* **2020**, *321*, 463.
[95] S. Qu, Y. Liu, Q. Hu, Y. Han, Z. Hao, J. Shen, K. Zhu, *J Control Release* **2020**, *321*, 710.
[96] P. Mittal, A. Saharan, R. Verma, F. M. A. Altalbawy, M. A. Alfaidi, G. E. S. Batiha, W. Akter, R. K. Gautam, M. S. Uddin, M. S. D. Rahman, *Biomed Res. Int.* **2021**, *2021*, 8844030.
[97] R. Karthikeyan, O. Koushik, P. Kumar, *Dendrimeric Architecture for Effective Antimicrobial Therapy*, 1st ed., Apple Academic Press, Florida **2018**,.
[98] A. Castonguay, E. Ladd, T. van de Ven, A. Kakkar, *New J. Chem.* **2012**, *36*, 199.
[99] G. Jiang, S. Liu, T. Yu, R. Wu, Y. Ren, H. C. van der Mei, J. Liu, H. J. Busscher, *Acta Biomater.* **2021**, *123*, 230.
[100] L. Zhang, D. Pornpattananangku, C.-M. J. Hu, C.-M. Huang, *Curr. Med. Chem.* **2010**, *17*, 585.
[101] L. Balogh, D. R. Swanson, D. A. Tomalia, G. L. Hagnauer, A. T. McManus, *Nano Lett.* **2001**, *1*, 18.
[102] A. A. Alencar de Queiroz, G. A. Abraham, M. A. Pires Camillo, O. Z. Higa, G. S. Silva, M. del Mar Fernández, J. San Román, *J. Biomater. Sci. Polym. Ed.* **2006**, *17*, 689.
[103] B. M. Discher, Y.-Y. Won, D. S. Ege, J. C.-M. Lee, F. S. Bates, D. E. Discher, D. A. Hammer, *Science* **1999**, *284*, 1143.
[104] F. Fenaroli, J. D. Robertson, E. Scarpa, V. M. Gouveia, C. Di Guglielmo, C. De Pace, P. M. Elks, A. Poma, D. Evangelopoulos, J. O. Canseco, T. K. Prajsnar, H. M. Marriott, D. H. Dockrell, S. J. Foster, T. D. McHugh, S. A. Renshaw, J. S. Martí, G. Battaglia, L. Rizzello, *ACS Nano* **2020**, *14*, 8287.
[105] M.-C. Jones, J.-C. Leroux, *Eur. J. Pharm. Biopharm.* **1999**, *48*, 101.
[106] R. Stancheva, T. Paunova-Krasteva, T. Topouzova-Hristova, S. Stoitsova, P. Petrov, E. Haladjova, *Pharmaceutics* **2023**, *15*, 1147.
[107] C. Y. Zhang, J. Gao, Z. Wang, *Adv. Mater.* **2018**, *30*, 1.
[108] M. Chen, S. Xie, J. Wei, X. Song, Z. Ding, X. Li, *ACS Appl. Mater. Interfaces* **2018**, *10*, 36814.
[109] H. Yoon, E. J. Dell, J. L. Freyer, L. M. Campos, W.-D. Jang, *Polymer* **2014**, *55*, 453.
[110] G. Wei, D. Nguyen, S. Reghu, J. Li, C. S. Chua, Y. Ishida, M. B. Chan-Park, *ACS Appl. Nano Mater.* **2020**, *3*, 2654.
[111] I. Insua, L. Zizmare, A. F. A. Peacock, A. M. Krachler, F. Fernandez-Trillo, *Sci. Rep.* **2017**, *7*, 9396.
[112] H. W. Lee, S. Kharel, S. C. J. Loo, *ACS Omega* **2022**, *7*, 35814.
[113] L. L. Li, J. H. Xu, G. B. Qi, X. Zhao, F. Yu, H. Wang, *ACS Nano* **2014**, *8*, 4975.
[114] X. Zhu, X. Chen, Z. Jia, D. Huo, Y. Liu, J. Liu, *J. Colloid Interface Sci.* **2021**, *603*, 615.
[115] D. P. Gnanadhas, M. Ben Thomas, M. Elango, A. M. Raichur, D. Chakravortty, *J. Antimicrob. Chemother.* **2013**, *68*, 2576.
[116] T. Niaz, A. Ihsan, R. Abbasi, S. Shabbir, T. Noor, M. Imran, *Int. J. Biol. Macromol.* **2019**, *138*, 1006.
[117] T. Niaz, S. Shabbir, T. Noor, R. Abbasi, M. Imran, *Int. J. Biol. Macromol.* **2020**, *156*, 1366.
[118] S. Javaid, N. M. Ahmad, A. Mahmood, H. Nasir, M. Iqbal, N. Ahmad, S. Irshad, *Polymers* **2021**, *13*, 2180.
[119] S. Abdelghany, T. Parumasivam, A. Pang, B. Roediger, P. Tang, K. Jahn, W. J. Britton, H. K. Chan, *J. Drug Deliv. Sci. Technol.* **2019**, *52*, 642.
[120] Y. Sun, A. Bhattacharjee, M. Reynolds, Y. V. Li, *J. Nanopart. Res.* **2021**, *23*, 1.
[121] A. Serri, A. Mahboubi, A. Zarghi, H. R. Moghimi, *J. Pharm. Pharm. Sci.* **2019**, *22*, 10.
[122] R. Maji, C. A. Omolo, N. Agrawal, K. Maduray, D. Hassan, C. Mokhtar, I. Mackhraj, T. Govender, *Mol. Pharm.* **2019**, *16*, 4594.
[123] S. Liu, X. Cai, W. Xue, D. Ma, W. Zhang, *Carbohydr. Polym.* **2020**, *234*, 115928.
[124] V. Viswanath, K. Santhakumar, *J. Taiwan Inst. Chem. Eng.* **2020**, *116*, 11.
[125] P. Walvekar, R. Gannimani, M. Salih, S. Makhathini, C. Mocktar, T. Govender, *Colloids Surf B Biointerfaces* **2019**, *182*, 110388.
[126] I. Insua, E. Liamas, Z. Zhang, A. F. A. Peacock, A. M. Krachler, F. Fernandez-Trillo, *Polym. Chem.* **2016**, *7*, 2684.
[127] R. Jijie, A. Barras, F. Teodorescu, R. Boukherroub, S. Szunerits, *Mol. Syst. Des. Eng.* **2017**, *2*, 349.
[128] Y. C. Yeh, T. H. Huang, S. C. Yang, C. C. Chen, J. Y. Fang, *Front. Chem.* **2020**, *8*, 286.
[129] A. Jung, Y. Jik, *J. Control Release* **2011**, *156*, 128.
[130] Z. Wang, K. Dong, Z. Liu, Y. Zhang, Z. Chen, H. Sun, J. Ren, X. Qu, *Biomaterials* **2017**, *113*, 145.
[131] P. J. Finley, R. Norton, C. Austin, A. Mitchell, S. Zank, P. Durham, *Antimicrob. Agents Chemother.* **2015**, *59*, 4734.
[132] C. P. Randall, A. Gupta, N. Jackson, D. Busse, A. J. O'Neill, *J. Antimicrob. Chemother.* **2015**, *70*, 1037.
[133] G. L. Burygin, B. N. Khlebtsov, A. N. Shantrokha, L. A. Dykman, V. A. Bogatyrev, N. G. Khlebtsov, *Nanoscale Res. Lett.* **2009**, *4*, 794.
[134] N. Rabiee, S. Ahmadi, O. Akhavan, R. Luque, *Materials* **2022**, *15*, 1799.
[135] M. Liu, D. He, T. Yang, W. Liu, L. Mao, Y. Zhu, J. Wu, G. Luo, J. Deng, *J. Nanobiotechnol.* **2018**, *16*, 1.
[136] N. Niño-Martínez, M. F. Salas Orozco, G.-A. Martínez-Castañón, F. Torres Méndez, F. Ruiz, *Int. J. Mol. Sci.* **2019**, *20*, 2808.
[137] N. Yu, X. Wang, L. Qiu, T. Cai, C. Jiang, Y. Sun, Y. Li, H. Peng, H. Xiong, *Chem. Eng. J.* **2020**, *380*, 122582.
[138] L. Wang, C. Hu, L. Shao, *Int. J. Nanomed.* **2017**, *12*, 1227.
[139] S. Bamrungsap, Z. Zhao, T. Chen, L. Wang, C. Li, T. Fu, W. N. Tan, *Nanomedicine* **2012**, *7*, 1253.
[140] J. Li, I. Mutreja, G. J. Hooper, K. Clinch, K. Lim, G. Evans, T. B. F. Woodfield, *Adv. Mater. Interfaces* **2020**, *7*, 1901963.
[141] Z. Yuan, S. Huang, S. Lan, H. Xiong, B. Tao, Y. Ding, Y. Liu, P. Liu, K. Cai, *J. Mater. Chem. B* **2018**, *6*, 8090.
[142] B.o Wang, N.a Zhang, W. Feng, S. Chen, X. Zhu, X. Shan, R. Yuan, B.o Yuan, H. Wang, G. Zhou, J. Liu, X. Sun, *Adv. Funct. Mater.* **2024**, *34*, 2407934.
[143] H. C. Zhou, J. R. Long, O. M. Yaghi, *Chem. Rev.* **2012**, *112*, 673.
[144] A. Wojciechowska, A. Gagor, W. Zierkiewicz, A. Jarząb, A. Dylong, M. Duczmal, *RSC Adv.* **2015**, *5*, 36295.
[145] H. D. Lawson, S. P. Walton, C. Chan, *ACS Appl. Mater. Interfaces* **2021**, *13*, 7004.
[146] X. Wang, P. C. Lan, S. Ma, *ACS Cent. Sci.* **2020**, *6*, 1497.
[147] X. Li, N. Semiramoth, S. Hall, V. Tafani, J. Josse, F. Laurent, G. Salzano, D. Foulkes, P. Brodin, L. Majlessi, N.-E. Ghermani, G. Maurin, P. Couvreur, C. Serre, M.-F. Bernet-Camard, J. Zhang, R. Gref, *Part. Part. Syst. Charact.* **2019**, *36*, 1800360.
[148] S. Peng, B. Bie, Y. Sun, M. Liu, H. Cong, W. Zhou, Y. Xia, H. Tang, H. Deng, X. Zhou, *Nat. Commun.* **2018**, *9*, 1.
[149] M. Liang, M. Zhang, S. Yu, Q. Wu, K. Ma, Y. Chen, X. Liu, C. Li, F. Wang, *Small* **2020**, *16*, 1905938.
[150] A. Karakeçili, B. Topuz, S. Korpayev, M. Erdek, *Mater. Sci. Eng. C Mater. Biol. Appl.* **2019**, *105*, 110098.

[151] X. Li, M. Qi, C. Li, B. Dong, J. Wang, M. D. Weir, S. Imazato, L. Du, C. D. Lynch, L. Xu, Y. Zhou, L. Wang, H. H. K. Xu, *J. Mater. Chem. B* **2019**, *7*, 6955.
[152] M. Liu, Y. F. Mu, S. Yao, S. Guo, X. W. Guo, Z. M. Zhang, T. B. Lu, *Appl. Catal. B* **2019**, *245*, 496.
[153] C. Tamames-Tabar, E. Imbuluzqueta, N. Guillou, C. Serre, S. R. Miller, E. Elkaïm, P. Horcajada, M. J. Blanco-Prieto, *Cryst. Eng. Comm.* **2015**, *17*, 456.
[154] M. Shen, F. Forghani, X. Kong, D. Liu, X. Ye, S. Chen, T. Ding, *Compr. Rev. Food. Sci. Food Saf.* **2020**, *19*, 1397.
[155] I. Ghaffar, M. Imran, S. Perveen, T. Kanwal, S. Saifullah, M. F. Bertino, C. J. Ehrhardt, V. K. Yadavalli, M. R. Shah, *Mater Sci. Eng. C* **2019**, *105*, 110111.
[156] Y. Sun, H. Zhao, F. Pu, H. Liu, L. Chen, J. Ren, X. Qu, *Adv. Healthcare Mater.* **2024**, *13*, 2400899.
[157] A. Nawaz, S. M. Ali, N. F. Rana, T. Tanweer, A. Batool, T. J. Webster, F. Menaa, S. Riaz, Z. Rehman, F. Batool, M. Fatima, T. Maryam, I. Shafique, A. Saleem, A. Iqbal, *Nanomaterials* **2021**, *11*, 3152.
[158] S. K. Jana, A. Gucchait, S. Paul, T. Saha, S. Acharya, K. M. Hoque, A. K. Misra, B. K. Chatterjee, T. Chatterjee, P. Chakrabarti, *ACS Appl. Bio Mater* **2021**, *4*, 3089.
[159] H. Gu, P. L. Ho, E. Tong, L. Wang, B. Xu, *Nano Lett.* **2003**, *3*, 1261.
[160] A. Masri, A. Anwar, D. Ahmed, R. B. Siddiqui, M. R. Shah, N. A. Khan, *Antibiotics* **2018**, *7*, 1.
[161] A. Kaur, S. Preet, V. Kumar, R. Kumar, R. Kumar, *Colloids Surf B Biointerfaces* **2019**, *176*, 62.
[162] S. S. Naqvi, H. Anwer, A. Siddiqui, R. R. Zohra, S. A. Ali, M. R. Shah, S. Hashim, *Plasmonics* **2021**, *16*, 1915.
[163] Z. Assadi, G. Emtiazi, A. Zarrabi, *J. Mol. Liq.* **2018**, *250*, 375.
[164] N. Huang, X. Chen, X. Zhu, M. Xu, J. Liu, *Biomaterials* **2017**, *141*, 296.
[165] M. Vahdati, T. Tohidi Moghadam, *Sci. Rep.* **2020**, *10*, 510.
[166] P. K. Tyagi, D. Gola, S. Tyagi, A. K. Mishra, A. Kumar, N. Chauhan, A. Ahuja, S. Sirohi, *Environ. Nanotechnol. Monit. Manag.* **2020**, *14*, 100391.
[167] R. Huang, G. Q. Cai, J. Li, X. S. Li, H. T. Liu, X. L. Shang, J. D. Zhou, X. M. Nie, R. Gui, *J. Nanobiotechnol.* **2021**, *19*, 1.
[168] Y. Xiao, M. Xu, N. Lv, C. Cheng, P. Huang, J. Li, Y. Hu, M. Sun, *Acta Biomater.* **2021**, *122*, 291.
[169] B. Soltani, H. Nabipour, N. A. Nasab, *J. Inorg. Organomet. Polym. Mater.* **2018**, *28*, 1090.
[170] D. Mao, F. Hu, Kenry, S. Ji, W. Wu, D. Ding, D. Kong, B. Liu, *Adv. Mater.* **2018**, *30*, 1706831.
[171] Y. Zhang, P. Sun, L. Zhang, Z. Wang, F. Wang, K. Dong, Z. Liu, J. Ren, X. Qu, *Adv. Funct. Mater.* **2019**, *29*, 1808594.
[172] S. Liu, L. Wei, L. Hao, N. Fang, M. W. Chang, R. Xu, Y. Yang, Y. Chen, *ACS Nano* **2009**, *3*, 3891.
[173] H. T. Nguyen, T. L. Ho, A. Pratomo, N. A. Ilsan, T. Huang, C. H. Chen, E. Y. Chuang, *Mater Sci. Eng. C* **2021**, *128*, 112265.
[174] H. Pandey, V. Parashar, R. Parashar, R. Prakash, P. W. Ramteke, A. C. Pandey, *Nanoscale* **2011**, *3*, 4104.
[175] C. M. Liauw, M. Vaidya, A. J. Slate, N. A. Hickey, S. Ryder, E. Martínez-Periñán, A. J. McBain, C. E. Banks, K. A. Whitehead, *Antibiotics* **2023**, *12*, 776.
[176] K. Krishnamoorthy, M. Veerapandian, L. H. Zhang, K. Yun, S. J. Kim, *J. Phys. Chem. C* **2012**, *116*, 17280.
[177] J. Liang, W. Li, J. Chen, X. Huang, Y. Liu, X. Zhang, W. Shu, B. Lei, H. Zhang, *ACS Appl. Bio Mater.* **2021**, *4*, 6937.
[178] R. Knoblauch, A. Harvey, E. Ra, K. M. Greenberg, J. Lau, E. Hawkins, C. D. Geddes, *Nanoscale* **2021**, *13*, 85.
[179] X. Wang, Q. Shi, Z. Zha, D. Zhu, L. Zheng, L. Shi, X. Wei, L. Lian, K. Wu, L. Cheng, *Bioact. Mater.* **2021**, *6*, 4389.
[180] H. Ji, K. Dong, Z. Yan, C. Ding, Z. Chen, J. Ren, X. Qu, *Small* **2016**, *12*, 6200.
[181] C. L. Zhu, X. W. Wang, Z. Z. Lin, Z. H. Xie, X. R. Wang, *J. Food Drug Anal.* **2014**, *22*, 18.
[182] M. Martínez-Carmona, Y. K. Gun'ko, M. Vallet-Regí, *Pharmaceutics* **2018**, *10*, 279.
[183] M. Gisbert-Garzarán, M. Manzano, M. Vallet-Regí, *Pharmaceutics* **2020**, *12*, 83.
[184] C. Xu, C. Lei, C. Yu, *Front. Chem.* **2019**, *7*, 290.
[185] J. Tu, A. L. Boyle, H. Friedrich, P. H. H. Bomans, J. Bussmann, N. A. J. M. Sommerdijk, W. Jiskoot, A. Kros, *ACS Appl. Mater. Interfaces* **2016**, *8*, 32211.
[186] A. Trofimov, A. Ivanova, M. Zyuzin, A. Timin, *Pharmaceutics* **2018**, *10*, 167.
[187] Y. Kuthati, P.-J. Sung, C.-F. Weng, C.-Y. Mou, C.-H. Lee, *J. Nanosci. Nanotechnol.* **2013**, *13*, 2399.
[188] G. Qi, L. Li, F. Yu, H. Wang, *ACS Appl. Mater. Interfaces* **2013**, *5*, 10874.
[189] Z. Gounani, M. A. Asadollahi, R. L. Meyer, A. Arpanaei, *Int. J. Pharm.* **2018**, *537*, 148.
[190] N. Velikova, N. Mas, L. Miguel-Romero, L. Polo, E. Stolte, E. Zaccaria, R. Cao, N. Taverne, J. R. Murguía, R. Martinez-Manez, A. Marina, J. Wells, *Nanomedicine* **2017**, *13*, 569.
[191] S. Wu, Y. Huang, J. Yan, Y. Li, J. Wang, Y. Y. Yang, P. Yuan, X. Ding, *Adv. Funct. Mater.* **2021**, *31*, 2103442.
[192] M. Colilla, M. Vallet-Regí, *Int. J. Mol. Sci.* **2020**, *21*, 1.
[193] X. Wang, L.-L. Tan, X. Li, N. Song, Z. Li, J.-N. Hu, Y.-M. Cheng, Y. Wang, Y.-W. Yang, *Chem. Commun* **2016**, *52*, 13775.
[194] X. Chen, Y. Liu, A. Lin, N. Huang, L. Long, Y. Gang, J. Liu, *Biomater. Sci.* **2018**, *6*, 1923.
[195] B. González, M. Colilla, J. Díez, D. Pedraza, M. Guembe, I. Izquierdo-Barba, M. Vallet-Regí, *Acta Biomater.* **2018**, *68*, 261.
[196] E. Krakor, S. Saniternik, I. Gessner, R. Frohnhoven, M. Wilhelm, M. Drexelius, N. Tosun, I. Neundorf, S. Mathur, *J. Am. Ceram. Soc.* **2021**, *105*, 1685.
[197] J. H. Choy, S. J. Choi, J. M. Oh, T. Park, *Appl. Clay Sci.* **2007**, *36*, 122.
[198] Y. Ping, X. Hu, Q. Yao, Q. Hu, S. Amini, A. Miserez, G. Tang, *Nanoscale* **2016**, *8*, 16486.
[199] M. Y. Memar, K. Adibkia, S. Farajnia, H. S. Kafil, S. Maleki-Diza, R. B. Ghotaslou, *J. Drug. Deliv. Sci. Technol.* **2019**, *54*, 101307.
[200] K. H. Min, E.-Y. Jang, H. J. Lee, Y.-S. Hwang, J.-I. Ryu, J.-H. Moon, S. C. Lee, *J. Ind. Eng. Chem.* **2019**, *71*, 210.
[201] H. Zhao, C. Zhao, Z. Liu, J. Yi, X. Liu, J. Ren, X. Qu, *Angew. Chem. Int. Ed.* **2023**, *62*, 202303989.
[202] D. L. Clemens, B. Y. Lee, M. Xue, C. R. Thomas, H. Meng, D. Ferris, A. E. Nel, J. I. Zink, M. A. Horwitz, *Antimicrob. Agents Chemother.* **2012**, *56*, 2535.
[203] R. J. Mudakavi, S. Vanamali, D. Chakravortty, A. M. Raichur, *RSC Adv.* **2017**, *7*, 7022.
[204] H. Devlin, S. Fulaz, D. W. Hiebner, J. P. O'gara, E. Casey, *Int. J. Nanomed.* **2021**, *16*, 1929.
[205] A. García, B. González, C. Harvey, I. Izquierdo-Barba, M. Vallet-Regí, *Microporous Mesoporous Mater.* **2021**, *328*, 111489.

Guillermo Landa received his PhD in Chemical Engineering and Environmental Technologies from the University of Zaragoza, Spain, where he is currently working as a Postdoctoral Researcher. His research is a continuation of his doctoral work and focuses on the development of nanotherapies for the treatment of bacterial infections, aiming to improve antimicrobial efficacy, reduce toxicity, and address antibiotic resistance.

Gracia Mendoza is Senior Researcher at Health Research Institute Aragon (IIS Aragon) in Zaragoza, Spain. She has authored several articles in journals such as Biomaterials, Small, and ACS Applied Materials and Interfaces, among others. Her research focuses on drug delivery systems with biomedical applications, mainly bactericidal nanomaterials and materials for the treatment of joint diseases.

Silvia Irusta is a Professor at the El Litoral University, Argentina (1985–2004). Researcher of the Consejo Nacional de Investigaciones Científicas y Técnicas, Argentina (CONICET) (1989–2004). Professor at University of Zaragoza (Spain). Member of the Institute of Nanocience and Materials of Aragon (Spain) (2004–2023). Research interests: Surface characterization of solids by XPS and FTIR spectroscopies. Polymeric nanocomposites. Synthesis of inorganic nanoparticles, nanotubes and nanofibers.

Manuel Arruebo is a Professor in Chemical Engineering in the University of Zaragoza, Spain. His research focuses on the synthesis and characterization of nanostructured materials including metal and polymer nanoparticles for drug delivery applications. He is also involved in developing antimicrobial nanostructured materials designed to prevent antibiotic resistance and minimize toxicity to human cells. His current research is focused on identifying new synergistic combinations of antimicrobials (or clinically approved drugs) together with nanoparticles and biologics (antimicrobial peptides or cell-derived exosomes) to shorten treatment, increase efficacy, reduce toxicity, prevent resistance, and treat infections caused by drug-resistant strains.